Limnol. Oceanogr., 51(2), 2006, 1107–1124

Physical pathways of nutrient supply in a small, ultraoligotrophic arctic lake during summer stratification

Sally MacIntyre[1]
Marine Science Institute and Department of Ecology, Evolution, and Marine Biology, University of California, Santa Barbara, California 93106

James O. Sickman
Marine Science Institute, University of California, Santa Barbara, California 93106-6150; and Soil and Water Science Department, University of Florida, Gainesville, Florida 32611

Sarah A. Goldthwait
Marine Science Institute, University of California, Santa Barbara, California 93106-6150

George W. Kling
Department of Ecology and Evolutionary Biology, University of Michigan, Ann Arbor, Michigan 48109

Abstract

During the ice-free period in the Arctic, the thermal structure and mixing dynamics of small lakes change with the passing of air masses. In Toolik Lake, Alaska, stable warm air masses during the ice-free season were associated with lake warming, daily winds were maximally 4–7 m s^{-1} for less than 12 h duration, lake numbers (L_N) varied daily between 2 and 80, and values of the coefficient of vertical eddy diffusivity ranged from molecular to 10^{-6} m^2 s^{-1}. For the 3-week warming period following ice-off, vertical mixing, which occurred primarily near the lake's sloping boundaries, supplied inorganic nitrogen only to phytoplankton in the chlorophyll maxima and only at rates sufficient to support 10–22% of their daily needs. In the upper water column, chlorophyll concentrations and primary productivity decreased by a factor of three relative to the maximum at ice-off. In contrast, during transitions between warm and cold air masses or the converse, wind speeds exceeded 5 m s^{-1} for over 1 d and L_N decreased to values of 3 or lower for periods of 1–2 d. In consequence, turbulence increased by one to two orders of magnitude, dispersing the chlorophyll maximum into multiple layers and increasing solute concentrations in hypolimnetic waters. Increased precipitation accompanied cold air masses, and in one case stream discharge of ~30 times base flow led initially to an overflow and subsequently to a metalimnetic intrusion with loading of inorganic nitrogen 10 times the daily needs of phytoplankton. Overall, the frequency with which frontal systems moved through the region determined the temporal variance in nutrient supply. Spatial variability within the lake was generated by the degree of penetration of incoming streams and the vertical layering of intrusions. These temporal events and the layers induced are hot spots of activity important for sustaining growth in oligotrophic lakes.

Small, dimictic lakes are a major feature of the landscape in the northern temperate zone and the Arctic. Numerous studies have focused on these lakes (e.g., Fee et al. 1992, 1994; Schindler et al. 1996; O'Brien et al. 1997), but few studies have tried to elucidate and quantify the major pathways for nutrient flux under variable weather conditions. Deciphering these pathways and determining the frequency of events that induce them is critical for understanding a variety of ecosystem processes, such as mixing dynamics and primary production.

A number of pathways have been identified for nutrient and particle transport in lakes (*reviewed in* MacIntyre and Jellison 2001). For internal pathways, wind-induced vertical mixing across the thermocline has often been assumed to be critical for nutrient flux, but its role varies with development of the internal wave field and gradients in nutrient concentration (Robarts et al. 1998; MacIntyre et al. 1999; MacIntyre and Jellison 2001). Tracer experiments (Quay et al. 1980) and calculated fluxes (Fee et al. 1994) in small, stratified lakes show the coefficient of vertical eddy diffusivity K_z within the thermocline to be on the order of molecular diffusivity of heat, implying limited flux of nutrients by turbulent mixing. However, in tundra regions, average wind speeds are typically higher than in the

[1] Corresponding author.

Acknowledgments

Financial support was provided by NSF grants DEB 9726932, DEB 0108572, and OCE 9906924 to S.M., and NSF grants OPP 9615949, OPP 9911278, and DEB 9810222 to G.W.K. and J.E. Hobbie. Logistic support was provided by the University of Alaska Toolik Lake field station. We thank Lorenz Moosmann for help with all aspects of the project; Brice Loose for programming and graphics; W.J. Shaw for programming; and Neil Bettez, Karen Jo Riseng, Karie Slavik, Chris Wallace, Jim Laundre, Matt Levine, S. C. Whalen, and Erica Gwynn for help with field sampling and chemical and biological analyses. We deeply appreciate Michael Head's cogent advice and logistical assistance with the SCAMPs. Constructive comments from two anonymous reviewers and discussions with Leon Boegman and J.M. Melack greatly improved the manuscript.

boreal forest (Rouse et al. 1997), and trees do not shelter the lakes, suggesting that vertical mixing may play a more important role at latitudes above the tree line. Additional internal pathways that may be important within small lakes include recycling coupled with resuspension at the sediment-water interface (Fee 1979), intrusions of nutrients from shallow regions to offshore waters due to spatially varying rates of cooling (James and Barko 1991), or convection due to heat loss (MacIntyre et al. 2002). External pathways include stream and groundwater inflows, rainfall, and atmospheric deposition. Stream inflows and rainfall have been shown to dominate over internal loading processes in small high-latitude lakes; the contribution from rainfall is more significant in boreal than in arctic lakes (Fee et al. 1994; Whalen and Cornwell 1985).

The degree to which storm events modify nutrient uptake and primary production depends upon the intensity of the storm and the flow paths that result, as well as the preconditioning of the phytoplankton. The influence of wind depends upon the degree of stratification and basin geometry. For the same wind speed and stratification, wind forcing will more likely induce turbulence in lakes with shallower epilimnia and longer fetch as quantified by the Wedderburn and Lake numbers, W and L_N, respectively (Imberger and Patterson 1990). For values of W or $L_N > 12$, wind stirs the upper portions of the epilimnia; for intermediate values the thermocline partially upwells; for low values ($\sim$1), the thermocline upwells to the surface; and for very low values ($\ll$1), the lake fully mixes (Spigel and Imberger 1980; Monismith 1985, 1986; Stevens and Imberger 1996; MacIntyre et al. 1999). L_N is the more appropriate index to use for lakes given their complex stratification and bathymetry. L_N is proportional to the coefficient of vertical eddy diffusivity K_z (MacIntyre and Romero 2000; Yeates and Imberger 2004). In ecological studies, L_N has been linked to shifts in species composition as a tropical lake alternated between well-mixed and stratified conditions (Boland and Griffiths 1995) and to nutrient flux supplying phytoplankton in the chlorophyll maximum (MacIntyre et al. 1999). In this latter study, calculated fluxes were significant after a wind event in which L_N was $\sim$2 for 8 h or more. How L_N differs as a function of prevailing air masses and how it relates to nutrient fluxes over a summer season have not been addressed in ecological studies.

The flow path of incoming streams depends on stream temperature relative to lake water (Fisher et al. 1979; Killworth and Carmack 1979; Nepf and Oldham 1997) and on hydrodynamics away from river inlets such as the internal wave field and temporary thermoclines (Fisher and Smith 1983). The impact of incoming streams on lacustrine productivity varies with nutrient loading, the depth of inflow relative to the euphotic zone (Englert and Stewart 1983; Vincent et al. 1991), and associated turbidity (Squires and Lesack 2002). However, aside from channelized lakes (Fisher et al. 1979), it is unclear exactly what pathways these inflows take and whether the incoming water will be rapidly dispersed or will persist as a definable structure. The flow path will determine the consequences of loading and, if persistent, the intrusions that form may become areas of intense biological activity, similar to the ''thin layers'' documented in fjords and coastal waters (Cowles and Desiderio 1993; McManus et al. 2003). How the persistence of these features is linked to changes in surface heating and cooling and wind forcing due to the prevalence of different air masses and resulting changes in L_N is unknown.

Diel heating and cooling over the lake and adjacent land and the passing of fronts ultimately control the nature of wind and temperature events as well as the rainstorms that discharge nutrients into lakes. This physical forcing is driven by long- and short-term changes in climate; for example, the Arctic Oscillation drives decadal-scale variations in warming in springtime throughout the Arctic because it determines whether high pressure zones are located in the Arctic Ocean or south of the Bering Strait (Overland et al. 2002). The location of these high pressure zones determines prevailing wind directions over land and whether air masses are warm or cold. It is unclear how, exactly, these different air masses, or the transitions between them, will affect storm events and physical processes in lakes. Thus, understanding lake functions such as primary productivity requires understanding the impacts of shifts in prevalent air masses, the disturbances induced, the interactions when disturbances co-occur, and the resultant pathways of nutrient supply.

To determine the pathways of nutrient flow into and within a small arctic lake during summer stratification and to address their impact on primary productivity, we characterized physical and chemical conditions of lake water and stream inflows in Toolik Lake, Alaska. We used temperature-gradient microstructure profiling for high-resolution measurements of lake temperature, conductivity, fluorescence, photosynthetically available radiation (PAR), and temperature gradients from which turbulence was quantified as the rate of dissipation of turbulent kinetic energy ε. Time series measurements of temperature allowed us to document the lake's thermal structure, calculate L_N, determine times of entrainment due to wind mixing or surface cooling, and compute the coefficient of eddy diffusivity (K_z). Rhodamine additions and microstructure profiles allowed us to determine depths of intrusions from groundwater and stream inflows. Profiles of nutrients and chlorophyll and measurements of primary production were used to determine the biological impacts of physical forcing. Our results show the temporal and spatial variability in pathways of nutrient loading and in-lake fluxes and indicate the potential for formation of areas of intense biological activity in association with stream and groundwater inflows.

Study site

Toolik Lake, Alaska (68°38′N, 149°38′W), in the northern foothills of the Brooks Range is a multibasin kettle lake with a surface area of 1.5 km^2, mean depth of 7.1 m, and maximum depth of 25 m (Fig. 1A). Previous studies describing thermal structure, primary productivity, seasonal changes in bacterial diversity, food web structure, and water chemistry include Whalen and Alexander (1984, 1986); Whalen and Cornwall (1985); Miller et al. (1986); O'Brien et al. (1997); Hobbie et al. (1999*a*,*b*); Kling et al. (1992*a*,*b*, 2000); Vincent and Hobbie (2000); and Crump et al. (2003). Air masses

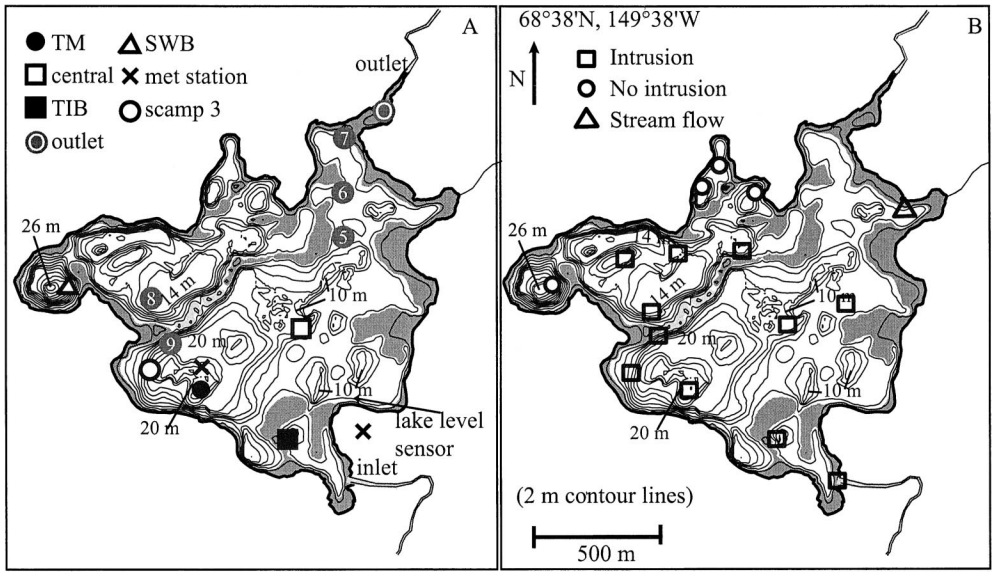

Fig. 1. (A) Bathymetric map and sampling stations of Toolik Lake. Contour intervals are 2 m, and shaded areas indicate moraines with water shallower than 3 m. Toolik Lake has a number of small basins (e.g., Toolik Inlet Bay [TIB] and South West Basin [SWB]) and a larger basin bisected by a moraine along the lake's northeast-southwest axis. South of this moraine is the ''main'' basin, which contains the Toolik Main (TM) site. Meteorological stations were located near Toolik Main and on the lake's southeast shore; one thermistor chain was near the meteorological station and one at the 10-m deep Central Station. Bottom slopes at TM were 0.005 m m^{-1} and near Central Station ranged from 0.01 to 0.04 m m^{-1}. The pressure transducer was located in a southeastern embayment marked with an arrow. SCAMP profiling was routinely conducted at TIB, TM, SWB, Central Station, and at an inshore station (scamp 3). The major inflow enters the lake from the south and exits to the north. Numbered stations and TIB, TM, Central Station, and near the outlet are locations where profiles of rhodamine and chlorophyll fluorescence were obtained on day 200. (B) Locations of SCAMP profiles on day 200 (19 July 1999). Open squares indicate locations where conductivities were reduced due to flow from inflow; open circles indicate locations where reductions were not observed, and the triangle indicated a location where SC was reduced but likely due to flow from a nearby inlet.

affecting local climate come from the Bering Sea to the southwest and from the Arctic front to the north. High winds are associated with the former and cold air masses with the latter (Miller et al. 1986). Due to high concentrations of chromophoric dissolved organic matter in the lake, attenuation of light is relatively high ($k_d \sim 0.5$ m^{-1}), although epilimnetic chlorophyll concentrations are low (2–4 μg chlorophyll *a* [Chl *a*] L^{-1} after ice-out in June; ~1 μg Chl *a* L^{-1} by midsummer; Miller et al. 1986). Soluble reactive phosphorus is supplied to the lake primarily during snowmelt and, due to retention in the sediments, does not accumulate in the water column during the winter. Inorganic nitrogen is also supplied mainly by allochthonous inputs, but some NH_4^+ is released from in-lake organic matter over the winter and nitrified, resulting in increasing concentrations of NO_3^- with depth at ice-off (O'Brien et al. 1997). The phytoplankton assemblage is diverse, with a high proportion of cryptophytes, chrysophytes, and chlorophytes (O'Brien et al. 1997; S. Holmgren pers. comm.). Annual primary productivity, which is based on measurements during the ice-free period, is quite variable, ranging from 1.7 to 11 g C m^{-2} yr^{-1} from 1975 to 1991, with a median value of 5.5 g C m^{-2} yr^{-1} (O'Brien et al. 1997). Primary productivity is highest just before and after ice-off (Miller et al. 1986), with nutrient limitation developing after ice-out in the upper water column (Miller et al. 1986; Levine and Whalen 2001).

Methods and calculations

Meteorological and radiation measurements—The meteorological station was on a floating platform anchored in the main basin of the lake (Fig. 1A). Wind speed and direction were measured with a Met One 014A anemometer 3 m above the lake surface; incoming and outgoing long- and short-wave radiation were measured with a Kipp and Zonen CNR1 net radiometer; relative humidity and air temperature were measured with a shielded and vented Vaisala HMP45C sensor. Each sensor was sampled every 5 s, and data were stored as 5-min averages. Water temperatures in the upper 5 cm were measured with a shielded self-contained temperature logger (Oregon Environmental Instruments OEI 9311, 0.005°C accuracy). A meteorological station on shore (Fig. 1A) measured PAR (Li-Cor Quantum sensor Model LI-190SB). Wind speed and direction (MET-ONE Model 014A) from that site were used on days 184–187 when the on-lake system failed. Wind speed from the two sites varies by <10%. Rain was measured with a tipping bucket rain gauge (Texas Electronics, Inc.) with 1% accuracy when rainfall ≤5 cm h^{-1}. Additional information on the Arctic LTER meteorological data is found at http://ecosystems.mbl.edu/ARC/data_doc/lanwater/climate/1999lwtlk_climate.html. Photosynthetic photon flux density was measured weekly with an underwater quantum sensor (LI-COR model LI-192SA sen-

sor, model LI-185 meter) at 0.5-m intervals and during profiles with the Self-contained Autonomous Microstructure Profiler (SCAMP; see below) and used to calculate the diffuse attenuation coefficient k_d using Beers Law. Lake surface elevation was measured with a pressure transducer (Druck, PDCR 930TI, full-scale 34.5 kPa + 0.5% giving a range of 0–3 m).

Time-series measurements of temperature—Time-series of temperatures were measured at two sites in the main basin; adjacent to the met station at Toolik Main (TM, nine depths); and at Central (8 depths) using self-contained temperature loggers on taut-line moorings with a subsurface float ~1 m below the air-water interface (Fig. 1A). Bottom slopes were low at TM. Central was selected as a site where the thermocline would come in contact with a sloping bottom boundary. Oregon Environmental Instruments (OEI) Model 9311 temperature loggers with an accuracy and resolution of 0.005°C and time constant of 5 s were used at TM. Recording was done at 10-s intervals. TSKA WaDaR loggers with an accuracy of 0.001°C, a resolution of 0.0014°C, and a time constant of ~3 min were used at Central. Recording was done at 30-s intervals. The units were calibrated before and after deployment against a platinum resistance thermometer with an accuracy of 0.0006°C. Data record is missing at Central for part of day 199 due to downloading of loggers.

Microstructure profiling—Temperature, temperature gradients, conductivity, fluorescence, PAR, and pressure were measured using temperature-gradient microstructure profilers (SCAMP, Precision Measurement Engineering; details in MacIntyre et al. 1999). Vertical resolution is 1 mm when falling or rising at 0.1 m s^{-1}. Sensors included two fast-response thermistors (FP07, time constant ~ 10 ms); a conductivity sensor located ~3 cm below the fast response sensors with a spatial resolution of ~1 cm; an LI-192SA Underwater Quantum Sensor for PAR; and a LED diode pair for chlorophyll fluorescence measurements. Excitation is by a blue, high-intensity LED that is wave-shaped to a narrow band of 455 + 60 nm via an optical interference filter. Emissions were filtered by a 685 nm interference filter and sensed by a broad-band photodiode. The depth transducer is ~0.65 m below the FP07 thermistors so the upper 0.65 m of the water column is not resolved on downcasts. Data from the fast response sensors were sharpened and smoothed digitally (Fozdar et al. 1985) before computing specific conductivity (SC, conductivity normalized to 25°C following Sengers and Watson 1986); density; and rates of dissipation of turbulent kinetic energy, ε. Calibrations were performed before and after the experiment. The reference thermometer was a Thermometrics TS8901, which has an accuracy of 0.005°C. Conductivity calibration was performed over the range 30–100 μS cm^{-1}.

Calibration of the SCAMP's fluorometer using discrete samples of chlorophyll obtained concurrently with the profiles was confounded in surface waters by nonphotochemical quenching during the day; below the chlorophyll maxima, values of chlorophyll were less per unit fluorescence than in the waters above. Hence, fluorescence values provide a measure of the fine-scale distribution of algal biomass rather than absolute Chl *a* concentration. Below 4 m depth, where photoinhibition was less, we obtained the regression Chl *a* (μg L^{-1}) = 3.87 V − 0.6, with r^2 = 0.6, where V is the output voltage of the fluorometer.

Rates of dissipation of turbulent kinetic energy ε, depths of isotherms, and L_N were computed as in MacIntyre et al. (1999). Hypsographic curves for the inlet basin, main basin, and entire lake were obtained by digitizing a bathymetric map of the lake. We used an atmospheric drag coefficient C_d at 10 m height of 1.3×10^{-3} and adjusted it to the height of the anemometer using law-of-the-wall scaling to compute air friction velocity, $u_* = (\rho_a/\rho_w\ C_d U^2)^{1/2}$, where ρ_a and ρ_w are density of air and water, respectively, and U is mean wind speed. Salinity was calculated as the sum of major ions in Toolik Lake using profile data from 1995 to 1998; specific conductivity was computed using these profiles of major ions and temperature following Wüest et al. (1996), and a linear regression between SC and salinity was used to convert SC from the SCAMP to salinity. Density using temperature and salinity was calculated following Chen and Millero (1977). The coefficient of eddy diffusivity K_z was calculated via analysis of SCAMP profiles following MacIntyre (1993), where R_f, the flux Richardson number used in the analysis, was calculated following Ivey et al. (1998). The buoyancy frequency, which is a measure of the density stratification, is calculated as $N = (g/\rho\ \partial\rho/\partial z)^{1/2}$. L_N was temporally filtered over 6 h because the significant timescale of wind forcing is one fourth the period of the dominant internal wave periodicity, 12–24 h in Toolik Lake. Lake-wide averaged K_z for the main basin was calculated as in Jassby and Powell (1975) with the 10-s thermistor string data bandpass filtered as required to avoid over- or underestimates of heat flux due to up- and downwelling of the thermocline from internal wave motions. The high-frequency cut off of the bandpass filter was set for 7 d by visual comparison of the filtered and measured temperature time series and used to describe the full time series and mean fluxes over weekly time periods. To accurately calculate fluxes over events of shorter duration, such as the low L_N events in midsummer, a filter cut off of 3 d best matched the time series temperatures.

Stream inflows—Water level of Toolik Inlet was determined by a Stevens Pulse Generator III and a float with data read by a Campbell Scientific CR10X data logger. Discharge was obtained using a rating curve derived with current speeds obtained with a Marsh-McBirney electromagnetic current meter. Conductivity and temperature were obtained with a Campbell 247 sensor with accuracy for conductivity of 10% in the range of 5 to 440 μS cm^{-1} and for temperature of 0.2°C. An intercomparison of this sensor with the SCAMP microconductivity sensor was not performed. Water for nutrient analysis was obtained with an ISCO sampler every ~3–6 h during rain events or high stream flow and at coarser intervals at other times. The flowpath of the inflowing stream in the lake was determined by dripping 4.5 L of Rhodamine WT into the stream water using a constant-head device (Mariotte bottle) on day 199 between 1340 and 1431 h, followed by measurements of in situ fluorescence obtained by pumping water from depth into a Turner Designs 10AU fluorometer equipped with flow-through cells with 10 ng L^{-1}

resolution. Fluorescence from phytoplankton was obtained in-line with a second fluorometer. Interference between rhodamine (excitation at 550 nm) and Chl *a* (excitation at 340–500 nm) was negligible, and the Turner 10AU was also effective in blocking turbidity interference (Robert Ellison, Turner Designs, pers. comm.). Profiles of conductivity taken by the SCAMP were also used to identify the flow path of the stream.

Chemical and biological analyses—Samples for nutrients were filtered in the field through Whatman GF/F filters. Ammonium and soluble reactive phosphate (SRP) were measured the day of collection; samples for NO_3^- were frozen and held in the dark before processing. Ammonium concentrations were measured fluorometrically (modified from Holmes et al. 1999). Internal standards were used to correct for matrix effects; final detection limit is ~0.1 μmol L^{-1}. Soluble reactive phosphate was measured with the molybdenum blue method (Strickland and Parsons 1972) with a detection limit of 0.05 μmol L^{-1}. Nitrate was measured using the cadmium reduction method on a Latchat Autoanalyzer (Johnson et al. 1985) within 3 months of sample collection (detection limit of 0.03 μmol L^{-1}). Samples for Chl *a* were filtered through Whatman 47 mm GF/C glass fiber filters within 2 h of collection and then extracted in buffered 90% acetone (1 mg L^{-1} $MgCO_3$) in the dark for 24 h. The concentration of Chl *a* was determined using a Turner Designs 10AU fluorometer with correction for pheophytin (Wetzel and Likens 2000). Samples for particulate C, N, and P were collected on precombusted GF/F filters. Particulate C and N were measured using an elemental analyzer. Particulate phosphorus was determined after sulfuric acid digestion (Stainton and Capel 1974). Alkalinity was determined using Gran titration (Stumm and Morgan 1981); in situ pH was measured with a Hydrolab SVR3-DL Surveyor 3 data logger and Hydrolab H20-BT-Std multiprobe. Dissolved inorganic carbon (DIC) was determined from pH and alkalinity (Kling et al. 1992*b*).

Primary productivity was evaluated by the ^{14}C method (Strickland and Parsons 1972) with incubations done in situ in 73-mL polystyrene tissue culture flasks. Two light and one dark bottle were incubated at each depth. Twenty-four hour incubations were performed at TM at 0, 1, 3, 5, 8, and 12 m. In addition, ^{14}C incubations for shorter periods were conducted at TIB, Central, TM, and SWB (Fig. 1A) to determine spatial variability in carbon uptake. At these stations, samples were typically incubated from four depths including near surface waters and the chlorophyll maximum. Variation was <30%. Incubations at TM and TIB were done from 14:30 to 21:00 h on day 189 and 17:20 to 21:20 h on day 199. Daily values for the shorter time periods were obtained by multiplying by daily irradiance divided by irradiance during the incubation. Areal primary production was computed for days when full profiles were obtained and corrected for the volume of the lake at each depth.

Results and interpretation

Lake physicochemical and biological conditions—Meteorology and lake thermal structure: Ice-off in 1999 occurred on day 172 (21 June) and was followed by a summer season marked by periods of heating interspersed with cold and warm fronts (Fig. 2). During the heating periods, incoming short wave radiation had daily maxima approaching 800 W m^{-2} (Fig. 2A), and wind speeds had a diel pattern with maximum winds generally in excess of 4 m s^{-1} rising by midafternoon and declining before midnight to speeds <1 m s^{-1} (Fig. 2B). Air temperatures typically varied 8–15°C over diel cycles (Fig. 3B) and relative humidity had daytime lows and nighttime maxima (Fig. 2D). The passage of cold fronts was marked by heavy cloud cover that dropped insolation below 400 W m^{-2} and winds from the north to northwest in excess of 5 m s^{-1} for at least 9 h and during more extreme events for over 24 h (days 187, 198 and 199, 201 and 202). Air temperatures dropped below surface water temperatures (Fig. 2C). The cold air masses persisted for 1–3 d, during which time relative humidity was always above 80% and the air was saturated in early morning (Fig. 2D). The highest winds of the summer (days 210–212) co-occurred with a transition to a warmer air mass and low relative humidity.

Rain or snow co-occurred with the cold air masses (days 186–189, 197–205, and 220–222; Fig. 3A). Co-incident with increased precipitation, stream temperature and SC decreased (Fig. 3B). Due to the cold front that passed through beginning on day 197, lake level rose and discharge increased to a peak of 16 m^3 s^{-1} (Fig. 3C). In addition, stream temperatures decreased from 17°C to 8.5°C; SC decreased from ~80 to 40 μS cm^{-1} (Fig. 3B); and NO_3^- and NH_4^+ concentrations increased to 3 μmol L^{-1} (Fig. 4). Concentrations of NO_3^- dropped while discharge was still low, whereas concentrations of NH_4^+ were still high at peak discharge; hence the maximum loading of NH_4^+ was 10 times higher than that of NO_3^-.

The upper mixed layer warmed from ice-out until day 197, cooled from day 197 until day 214, and warmed again after day 214 (Fig. 5B). During the early heating period, a shallow epilimnion with depth <3 m rapidly developed. Temperatures increased from 6°C to 18°C, and except on cloudy days, the epilimnion heated and cooled by 1°C on a daily basis. Once established, the metalimnion was exceptionally strongly stratified, with temperatures decreasing 6°C from 2 to 5 m, and the buoyancy frequency ranged from 0.05 to 0.07 s^{-1} (30 to 40 cycles per hour, cph), with values occasionally as high as 0.11 s^{-1} (65 cph). The diurnal winds forced internal waves with displacements of up to 1 m in the more highly stratified upper metalimnion, 2 m at its base, and up to 3 m in the hypolimnion (Fig. 5B). After the initial rapid setup of the thermocline, the isotherms descended gradually due to slow warming of the metalimnion.

The cold air temperatures, low insolation, and winds on day 198 marked the onset of a rapid transition to a cooling period with increased stream discharge. Diel heating and cooling of the epilimnion was muted if not stopped, and epilimnetic temperatures decreased 2°C on day 198 and continued to decrease on day 199. The incoming stream water was initially an overflow (see below); it became a metalimnetic intrusion and reduced the stratification in the metalimnion beginning on day 199. The intrusion can be recognized by the separation between the 10°C and 12°C isotherms (3–6 m depth) beginning on day 199 (Fig. 5B).

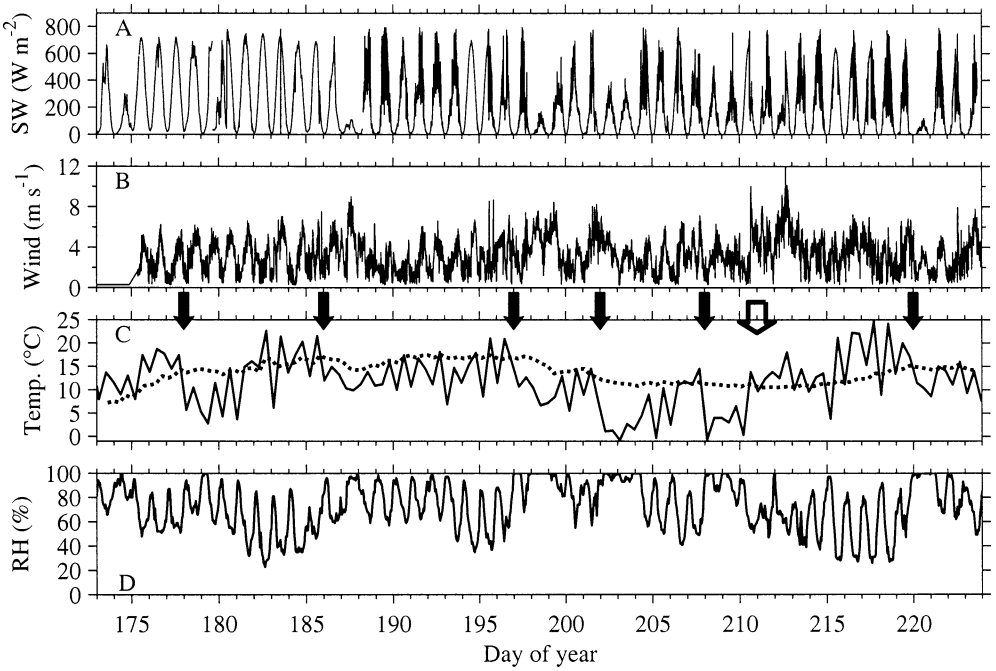

Fig. 2. (A) Incoming short-wave radiation, (B) wind speed, (C) air (solid line) and surface water (dotted) temperatures, and (D) relative humidity from day 172 (21 June 1999) to day 224 (12 August 1999). Surface water temperatures were measured by a self-contained temperature logger at 0.05 m depth. Onset of cooling periods (black arrows) and onset of warming period (white arrow). Decreased insolation, higher winds, and higher relative humidity were associated with the passage of colder air masses.

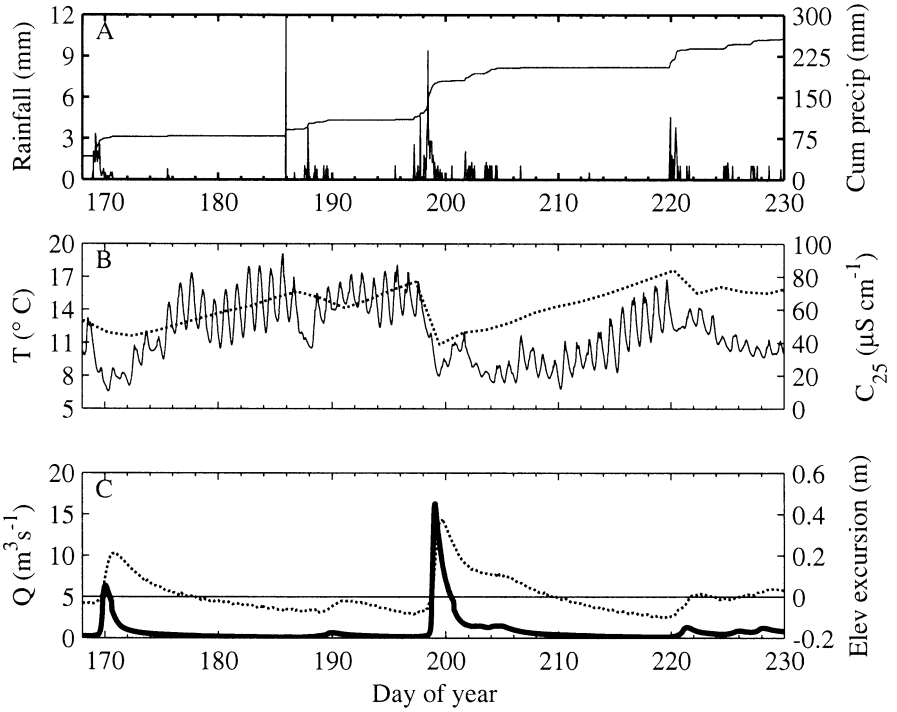

Fig. 3. (A) Rainfall and cumulative rainfall; (B) specific conductivity SC (μS cm^{-1}, dotted line) and temperature of Toolik Inlet; and (C) discharge (Q) of Toolik Inlet and change in lake surface elevation (dotted line) measured from day 169 (18 June 1999) through day 230 (18 August 1999).

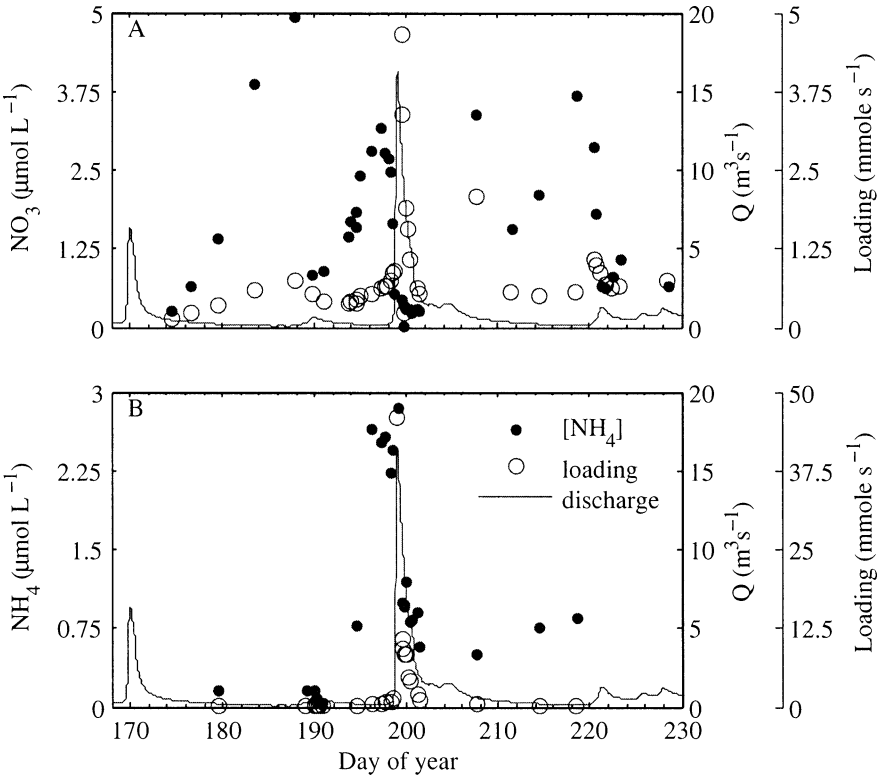

Fig. 4. (A) Discharge (Q) , concentration of NO_3^-, and loading of NO_3^- in Toolik Inlet for time period in Fig. 3; (B) as in (A) but for NH_4^+.

The combination of moderate winds, arrival of a second cold air mass, and low insolation after the inflow event led to deepening of the epilimnion to 5.5 m by day 204. Weak stratification persisted at the base of the epilimnion at least until day 207, indicating that it took at least a week for waters that had flowed into the metalimnion to be mixed into the epilimnion.

The Lake number L_N had daily lows ranging from 2 to 80 during the heating period (Fig. 5A). L_N dropped below 3 for longer periods in association with the cold fronts on days 187, 198–199, and 202 and decreased below 1 in association with the high winds on day 212. Abrupt deepening of the metalimnion and warming of metalimnetic and hypolimnetic waters occurred when L_N remained below 3 for over 24 h (e.g., days 201–202 and 212–213).

During periods when L_N was <6 for periods of at least 2 d either due to weak stratification (e.g., cold fronts) or sustained winds, average K_z values were lower (Fig. 5C). During the initial setup of the thermocline, the water column was turbulent as indicated by K_z up to 10^{-5} m^2 s^{-1}. From day 182 until day 195 when considerable epilimnetic heating occurred and L_N decreased below 6 for short periods, K_z ranged from molecular to $\sim 10^{-6}$ m^2 s^{-1}. From day 195 until 205, several periods of sustained winds occurred with $L_N <$ 3 for 24 h or wind direction along the long axes of the lake, and K_z was consistently higher with maxima of 3×10^{-6} m^2 s^{-1}. On days 210–213 when L_N was <3 for two 24-h periods (minimum of 0.8), K_z increased to $\sim 10^{-5}$ m^2 s^{-1} and the thermocline descended.

Seasonal time series of conductivity and fluorescence at Toolik Main—The water column was stratified chemically throughout the ice-free season (Fig. 6A). SC had a minimum centered around 8 m beginning with the first SCAMP casts on day 178, which persisted until the large storm event on day 198. Changes induced by the increased discharge from the storm included (1) decreased SC in the upper 5 m on day 199, (2) decreased SC between 2 and 6 m on day 200, and (3) increased SC below 10 m depth beginning on day 199. The first two changes indicate that the incoming stream water initially was an overflow and subsequently an underflow. These interpretations are supported by the decrease in temperature of the inflow, but as shown later, the mixing dynamics in the inlet basin are also important. Direct precipitation was $<2\%$ of the epilimnetic volume and insufficient to lower SC. The third change indicates that waters of higher conductance near the lake bottom were mixed vertically within the hypolimnion and into the lower metalimnion.

The chlorophyll maximum, as indicated by in vivo fluorescence (Fig. 6B) and chlorophyll profiles (Fig. 7A), was located between the 5 and 10°C isotherms (~5–10 m depth) and descended with them over the season (Fig. 6B). Maximum biomass reached 5 μg L^{-1}. Prior to day 199 the chlorophyll maximum extended throughout the main basin and biomass was higher in the sheltered basins (up to 8 μg L^{-1}). At the time of high inflow, fluorescence increased where SC decreased (Fig. 6), suggesting an inflow of algal biomass

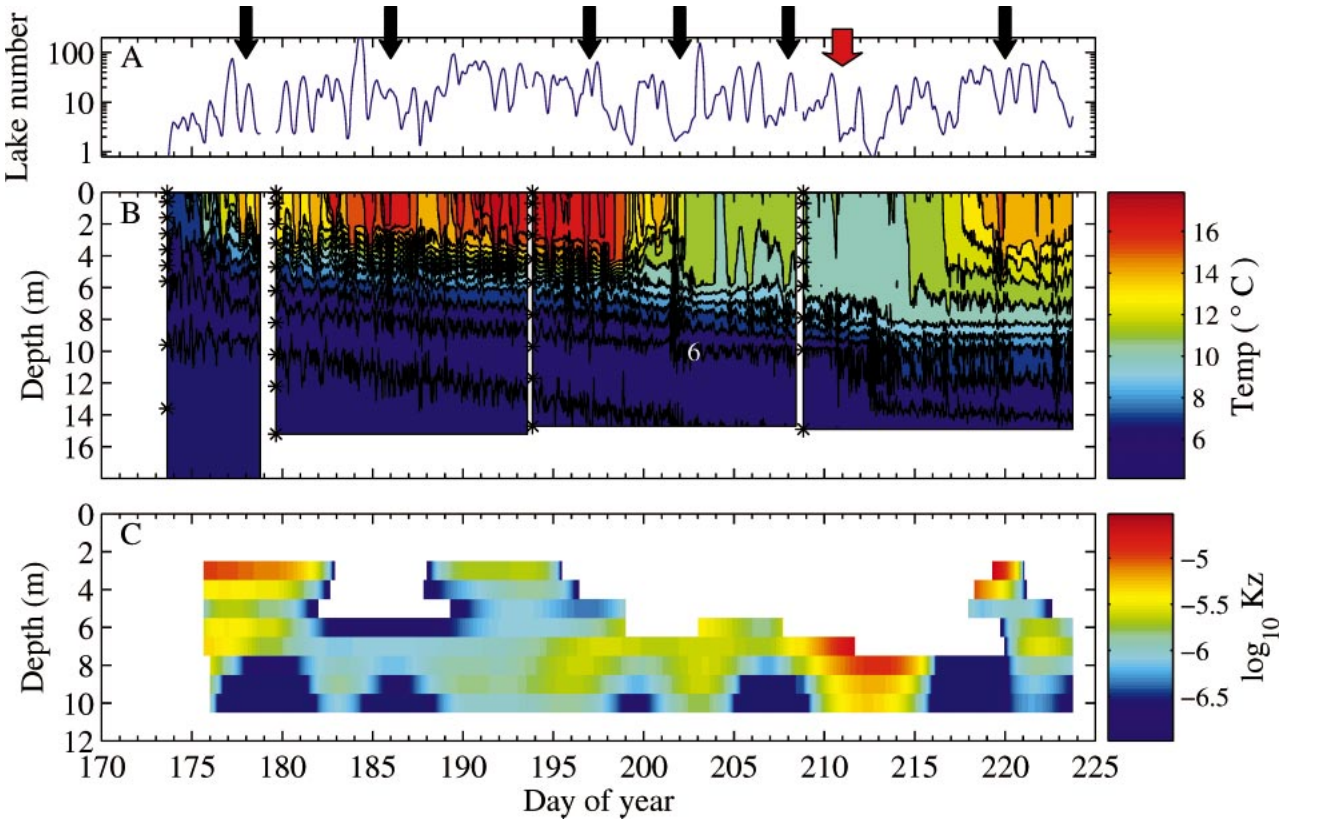

Fig. 5. (A) Lake number, (B) isotherms indicating thermal structure, and (C) logarithm of the coefficient of eddy diffusivity K_z (m^2 s^{-1}) at Toolik Main for time period in Fig. 2. Contour intervals for isotherms are 1°C; 6°C isotherm is labeled. Data are block averaged over 6-min intervals. Asterisks indicate depths of temperature loggers. K_z was obtained by filtering over 7 d. Black arrows indicate onset of cold front; red arrow indicates onset of a warm front.

into the main basin. The original chlorophyll maximum was diminished.

Microstructure profiles—Selected microstructure profiles taken before, during, and after the high stream inflows are shown for Toolik Inlet Bay (TIB; Fig. 8), TM (Fig. 9), and central (Fig. 10). The profiles taken before the storm (Figs. 8A, 9A, and 10A) are representative of conditions during the heating period showing strong thermal stratification and a conductivity minimum and chlorophyll maximum near 7 m. In the following, we describe physical changes at the inlet basin, TM, and the central station due to increased inflow from the storm. Initial mixing occurred in the inlet basin where, 12 h after peak storm discharge (day 199, 12:24 h), temperature, SC, and fluorescence were nearly uniform below 3 m depth and the entire water column was turbulent (Fig. 8B). Below 3 m, temperatures had declined to ~10.5°C and SC to 46 μS cm^{-1}. The following day, temperature, fluorescence, and SC showed more structure below 3 m. The cooler temperatures and increase in thermal stratification below 2 m on day 200 suggest that the stream inflow had penetrated to different depths at different times (Fig. 8C). The higher temperatures and SC in the upper 2 m on day 200 in comparison with day 199 suggest a backflow of water from the main basin, where temperatures and SC were higher (Figs. 9C,D, 10C).

The flow path of the inflow in the main basin varied over space and time during the first 2 d after peak discharge. The decrease in SC in the upper 4 m at TM on day 199 (12:48 h) relative to the prestorm period indicates that the inflow was initially an overflow (Fig. 9B). As stream temperatures decreased, the inflow became an intrusion within the metalimnion; the tongues of low conductance water at 5 m at 12:48 h and at 5 and 6.5 m at 16:55 h are indicative of the deeper inflows (Fig. 9B,C). ε was elevated within or on the boundaries of some of the intrusions (Fig. 9C). On day 200, the inflow intruded between 2 and 6.4 m at TM, as shown by the thicker layer of water with low SC (Fig. 9D). However, the plume was not yet uniform and the intrusion had three distinct steps in SC and temperature. The elevated turbulence ($\varepsilon = 10^{-6}$ m^2 s^{-3}) in the uppermost layer indicates shear either from inflowing water or tilting of the thermocline bordering the intrusion. The lowest value of SC was associated with the coolest temperature range. These variations in temperature and SC suggest that incoming water flowed to different depths at different times due to density differences induced by changes in incoming stream temperatures and mixing with different strata of the inlet basin.

The lower SC in the intrusion at the Central Station than at TM 13 h after peak discharge (Fig. 10B) and on day 200 (Fig. 10C) suggests that more of the intrusion was directed northward toward the outlet, rather than westward across the

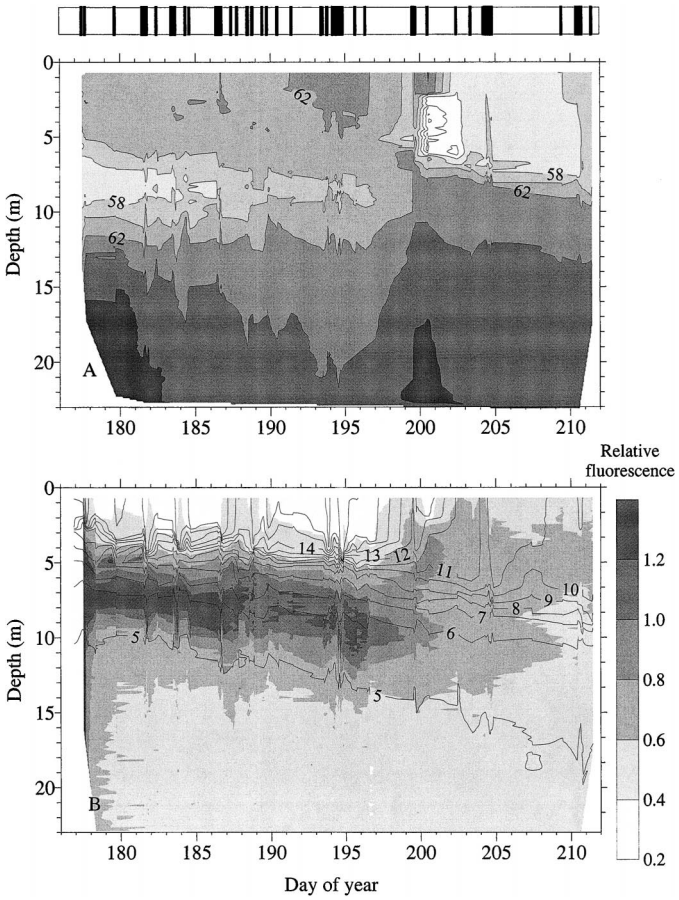

Fig. 6. (A) Time series of specific conductance (μS cm^{-1}) based on SCAMP casts at Toolik Main showing the initial conductivity minimum centered at 8 m depth and the intrusion of fresher water between 2 and 6 m depth due to the high discharge beginning on day 198. Times of SCAMP casts are shown in overlay. (B) Time series of relative fluorescence (volts) overlain on isotherms computed from profiles with the SCAMP.

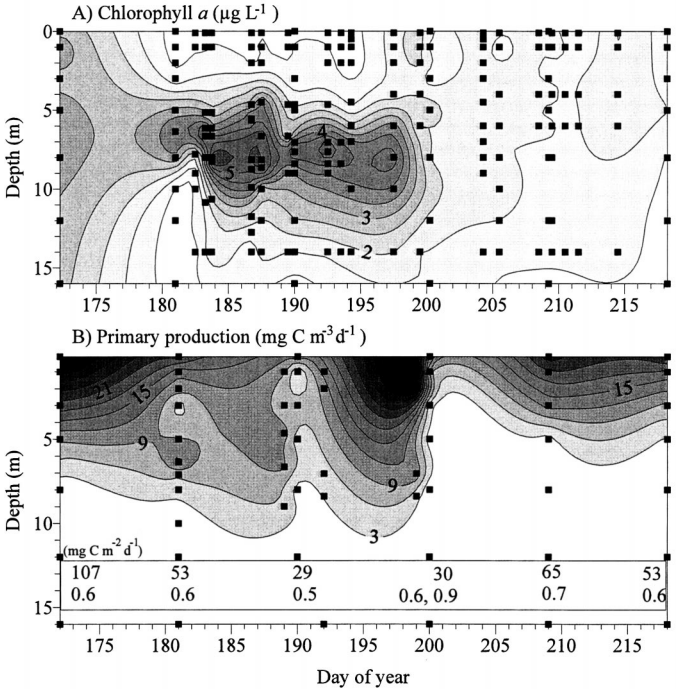

Fig. 7. (A) Total Chl *a*. (B) Primary productivity (mg C m^{-3} day^{-1}; shaded contours), and, within the rectangle at the bottom, areal primary productivity (mg C m^{-2} d^{-1}) and diffuse attenuation coefficients (m^{-1}), illustrating higher primary productivity at ice-off and when surface overflow occurred in Toolik Main. Filled squares indicate times and depths of sampling.

main basin of the lake (Fig. 1A). Turbulence was enhanced ($\varepsilon \sim 10^{-7}$ m^2 s^{-3}) and turbulent eddies were 5–10 cm in diameter (not shown) in the 2.5 m above the benthic boundary (Fig. 10B). In contrast, ε was lower in the intrusion than in the water above and below.

The storm led to a reduction in the chlorophyll maximum at TM and to development of multiple fluorescence peaks up to 1 m in vertical extent (Fig. 9B–D). The peaks observed at 12:48 h on day 199 occurred below the depth of the inflow and were likely due to fragmentation of the chlorophyll maximum by the turbulence associated with the low L_N at that time. On day 200 (Fig. 9D), fluorescence increased between 3.5 and 5 m at TM, and a similar increase was noted in the upper portion of the intrusion at the Central Station (Fig. 10C). At both stations, the increase occurred where temperatures were similar to those of the mixed water in TIB, ~11°C. This coincidence suggests that biomass was being transported from TIB. However, integrated biomass within TIB and in situ production were too low to account for the chlorophyll peaks. Thus, biomass transported from upstream lakes in the Toolik catchment likely contributed to the peak.

Microstructure profiles taken after day 200 indicate that 5 d were insufficient for complete mixing of the plume with ambient lake water in the midlake stations. The decrease in conductivity from the inflowing water was discernible in the epilimnion and the metalimnion on day 202 (Fig. 9E). Although the upper water column was well mixed to a depth of 4 m on day 204, structure in SC and fluorescence was still present to 7 m (Figs. 9F, 10D).

Horizontal distribution of the inflowing water—Lake-wide microstructure sampling (Fig. 1B) on the afternoon of day 200 documented intrusions of lower conductivity water at all locations except SWB and on the far northwestern side of the lake. SC in the intrusion was 10 μS cm^{-1} lower than SC of surface waters in the main basin but only 4 μS cm^{-1} lower than surface waters on the northwestern side of the lake.

Rhodamine was added to the inlet stream at ~14:00 h on day 199, and lake-wide samples were taken between 14:00 and 20:00 h on day 200 (Fig. 1A). Rhodamine was detected in TIB, at all our sampling stations in the main basin, but not at station 8 to the west of the main basin. The comparison of SC and tracer measurements indicates that at high discharge stream water crossed the moraine that transects the main basin (lower SC observed), but during falling discharge the intrusion was within the metalimnion and did not penetrate across the moraine (no rhodamine observed). Rhodamine concentrations were highest between 2.5 and 6 m and ranged from 0.04 μg L^{-1} at TM and Central, 0.02 μg L^{-1}

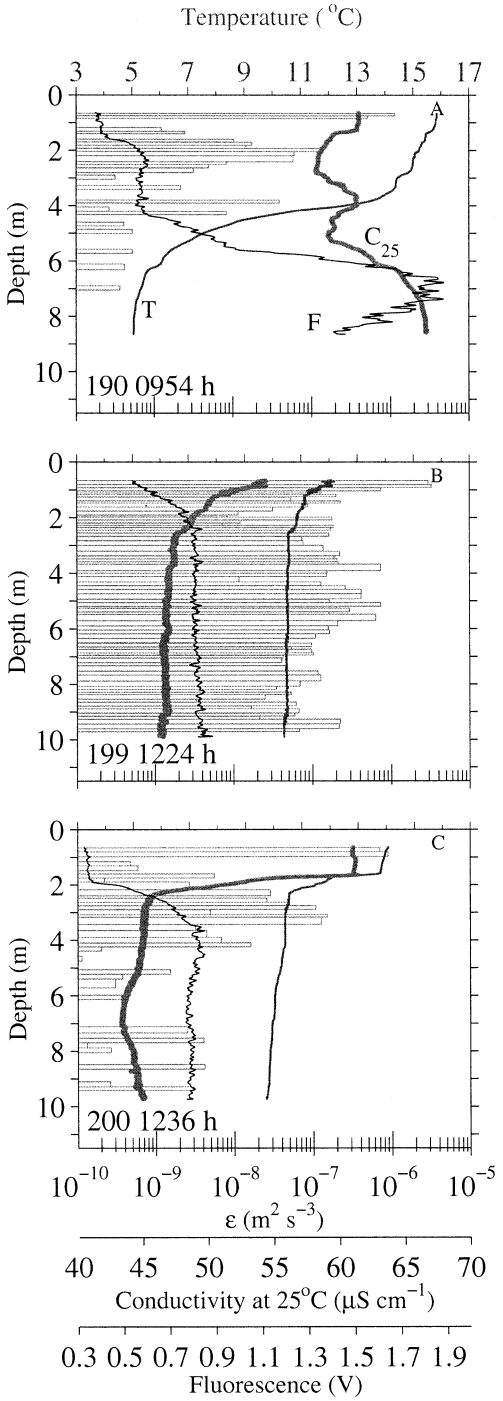

Fig. 8. Profiles of temperature T, SC (C_{25}), relative fluorescence F (volts), and rates of turbulent kinetic energy dissipation (ε, histograms) in Toolik Inlet Bay (A) on day 190 representing conditions before the rain event, (B) day 199 when discharge was maximal, and (C) day 200.

at station 9, 0.015 μg L^{-1} at station 5, and 0.005 μg L^{-1} at station 7. Chlorophyll fluorescence measured at the same time was elevated between 4 and 6 m, a similar depth range to the fluorescence peak in Fig. 9D attributed to the introduced phytoplankton. Rhodamine showed more pronounced layering at TM, Central, and station 9 than did chlorophyll fluorescence, again indicating vertical variability in depth of intrusions of different constituents. Based on a distance of 1.75 km from the mouth of the inlet to station 7, at least one part of the stream inflow moved at a mean speed of 1.5 cm s^{-1}.

Seasonal changes in nutrient concentrations, algal biomass, particulates, and seston ratios—Prior to the storm, concentrations of NH_4^+, NO_3^-, and SRP were near the limits of detection in the upper 10 m (Fig. 11). In response to the storm, increases in NH_4^+, NO_3^-, and SRP could be detected in surface waters. The largest increases in NH_4^+ occurred in the upper 2 m, and the largest increase in SRP occurred at 5 m. These differences indicate the changing depth of the intrusion over time and the different timescale of loading of different constituents. Unfortunately, NH_4^+ concentrations were not measured below 6 m during the inflow event, but on days 205 and 209 the nutricline was at 6 m depth and concentrations below 12 m were the highest recorded for the season.

Similarly to nutrients, concentrations of different particulates increased at different depths during the storm (not shown). At 3 m, particulate C increased from 24 to 36 μmol L^{-1} and particulate N increased from 3 to 5 μmol L^{-1}. C : Chl ratios > 360, PC : PN < 8.3, PN : PP > 40, and PC : PP > 250 indicate that a large fraction of this material was particulate organic matter high in nitrogen content but low in phosphorus. The departure of the stoichiometry from Redfield indicates that some portion of the introduced material was due to scouring of the inlet stream. In consequence, k_d increased in the water column from 0.6 m^{-1} on day 199 to 0.9 m^{-1} on day 200. Ten days later, the highest particulate concentrations and highest C : Chl ratios were between 6 and 10 m, indicating settling of a considerable fraction of the introduced organic material; k_d decreased to 0.7.

The bulk of the detrital material brought into the lake during spring runoff settled within 10 d of ice-out. Thus we use the particulate nutrient data as an indicator of the physiological state of the phytoplankton. From ice-off until before the storm, C : Chl ratios > 280 and PC : PN > 8.6 indicated phytoplankton in the upper water column were light- and nutrient-stressed (Guildford and Hecky 2000; Jellison and Melack 2001). In contrast, lower C : Chl and PC : PN $<$ 8.6 in the chlorophyll maximum indicated healthier phytoplankton within the metalimnion. PN : PP < 22 and PC : PP < 129 throughout the water column indicate that phytoplankton were P sufficient on day 181. Increases in these two ratios above critical values below 1 m indicate that moderate P limitation had developed in most of the water column by day 191. PN : PP < 22 between 5 and 8 m on day 200 indicated a reduction in P limitation in response to the storm.

Temporal changes in primary production—Both volumetric and areal primary production were relatively high at ice-off (107 mg C m^{-2} d^{-1}; Fig 7B). Subsequently, areal productivity decreased to 29 mg C m^{-2} d^{-1} as nutrient limitation increased. During the initial phase of high discharge, volumetric productivity increased at TM and TIB to values

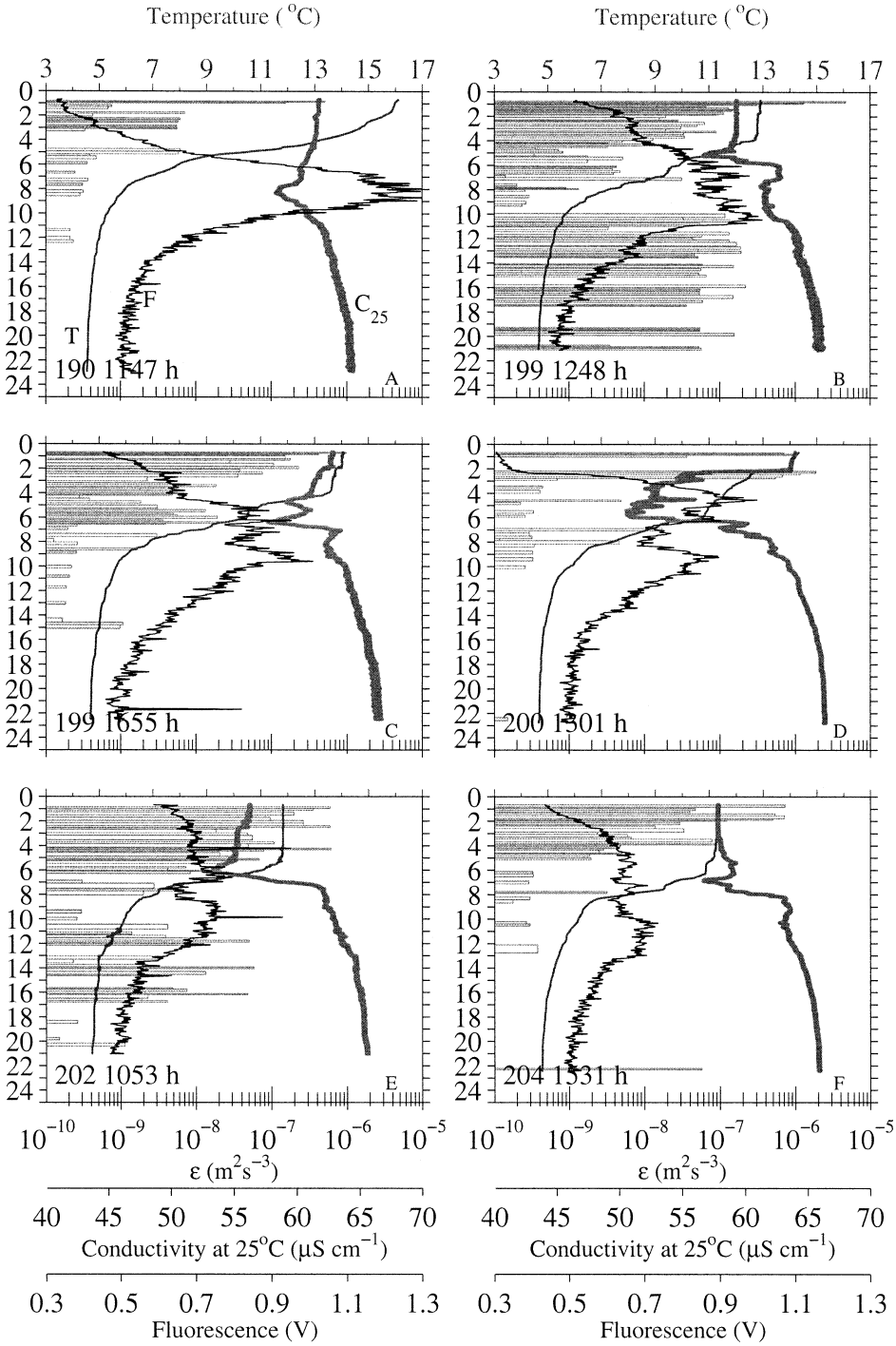

Fig. 9. As in Fig. 8 but at Toolik Main illustrating (A) the highly stratified conditions before the inflow event, changes after the inflow including (B) the reduction of stratification of surface water and fragmentation of the chlorophyll maximum, (B,C) intrusive flows with lower SC in the metalimnion, (D) a new layer with elevated fluorescence in the inflowing water, and (E,F) persistence of structure in the upper 6 m 3 and 5 d after the inflow.

exceeding those at ice-off. Areal productivity immediately after the storm was 30 mg C m^{-2} d^{-1}. Reductions in light from increased turbidity and color brought in by the inflow (extinction coefficient increased by 66%) may have contributed to the lower areal productivity. Spatial and temporal variability in the distribution of the inflowing stream water was likely more important. On day 200, algal biomass in the upper 3 m at TM was lower than on day 199 and SC was higher (Figs. 7A and 9B,C,D), whereas chlorophyll fluorescence was higher in the upper 3 m at Central (Fig. 10C).

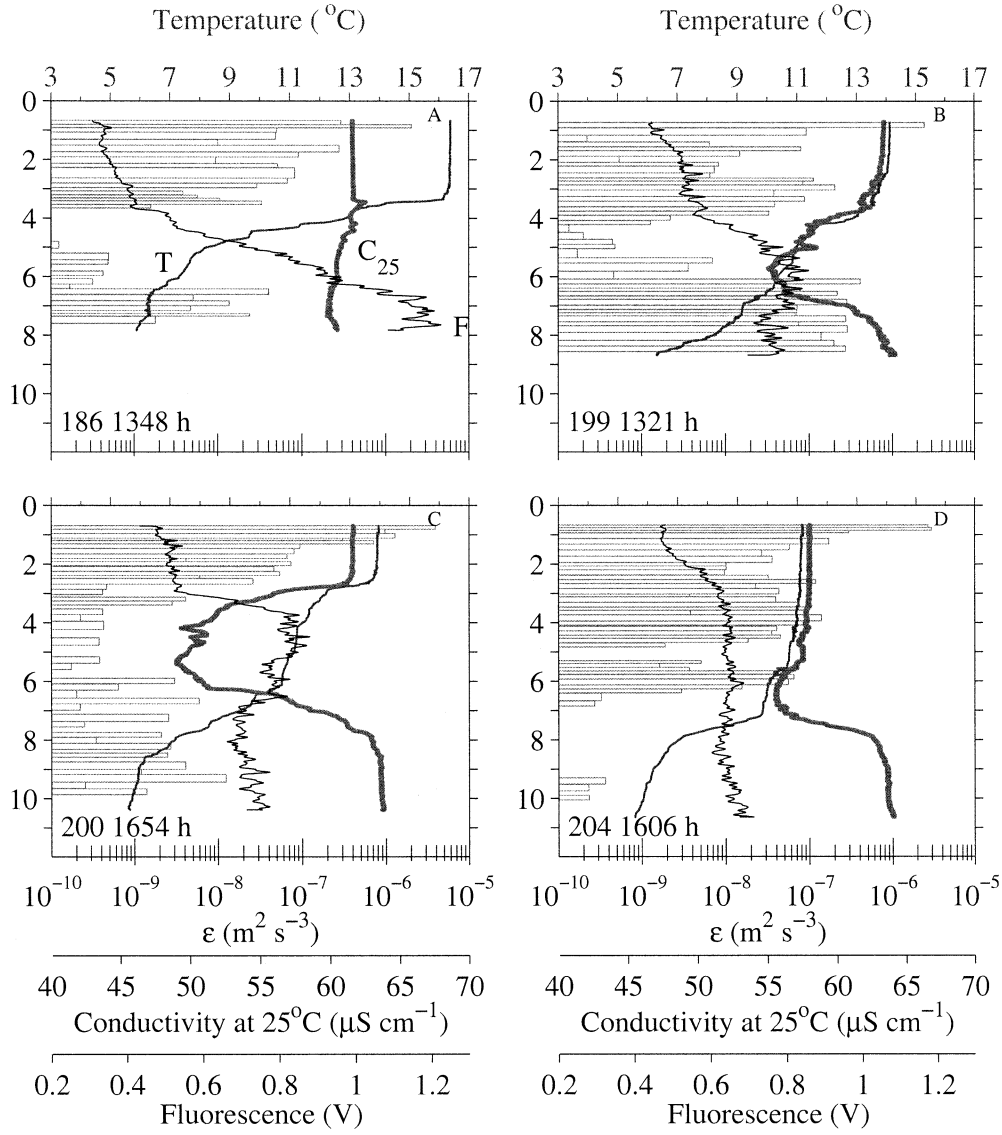

Fig. 10. As in Fig. 8 but at the Central Station illustrating (A) the initial highly stratified conditions, (B,C) the lower SC than at TM, (B) the enhanced turbulence in near bottom waters, (C) the increased chlorophyll fluorescence at the depth of the intrusion, and (F) persistence of structure after the event.

The temporal differences at TM indicate advection of water from regions of the lake not initially affected by the inflow. The spatial variations in biomass created the potential for spatial variability in primary productivity. After day 200, chlorophyll biomass was higher at TM and the transparency of the lake increased; on day 209, areal production was twice that in the period before the storm. Prior to the storm, photosynthetic efficiency, estimated as carbon uptake normalized to Chl *a* and daily irradiance at the depth of incubation, ranged from 0.025 to 0.11 μg C per μg Chl *a* per day per μmol quanta (m^{-2} s^{-1}) between 3 and 6 m. At these depths photosynthesis was light undersaturated for a significant portion of the day. In contrast, on days 199 and 200 and in the following week, photosynthetic efficiency at those depths increased to 0.16–0.18 μg C μg Chl a^{-1} d^{-1} (μmol quanta [m^{-2} s^{-1}])$^{-1}$, indicating that the growth capacity of phytoplankton had increased in response to the event.

Nutrient fluxes from vertical mixing and the stream inflow

The meteorological and temperature data indicate that prevailing air masses and the passage of fronts lead to distinct physical regimes at Toolik Lake during the summer. When warm air masses predominate, the lake accumulates heat, L_N only infrequently decreases to values below 10 and for periods typically shorter than 9 h, and vertical mixing is limited. In contrast, when colder air masses move into the region, the lake cools, precipitation occurs, and wind events persist for longer times. When cool periods persist, the density gradient across the top of the metalimnion is reduced, priming the lake to be more responsive to strong winds. Persistent wind forcing, from the arrival of another cold air mass or a warm one, leads to lower L_N for longer periods. In consequence, turbulence is enhanced by one to two orders

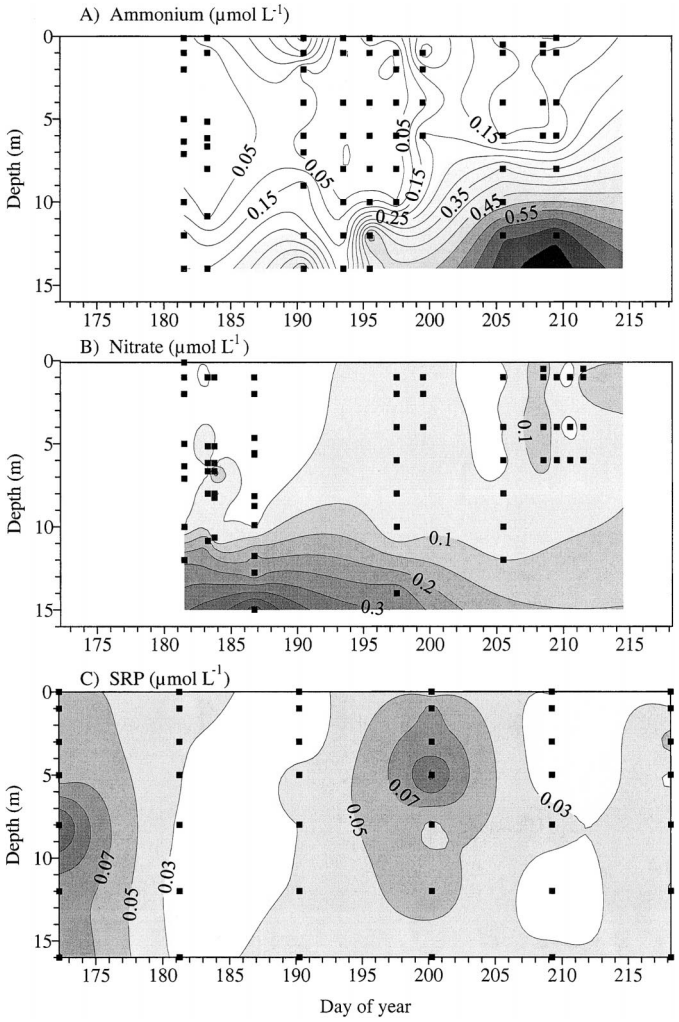

Fig. 11. (A) Ammonium, (B) nitrate, and (C) SRP at Toolik Main from day 181 (30 June 1999) to day 218 (6 August 1999) showing a nutricline below 10 m for N but not for P before the storm, and the increases of nutrients at different depths in association with the inflow on days 199 and 200. Filled squares indicate dates and depths of sampling.

of magnitude in the metalimnion and greater vertical mixing occurs.

Fluxes of N during the heating period—The nitricline was deep in the water column during the heating period, and the chlorophyll maximum and the nitricline were separated by 1–2 m in the vertical at TM. In such situations, partial upwelling, as described by Monismith (1986), of the nitricline at lateral boundaries combined with vertical mixing is required for transport of inorganic nitrogen to the chlorophyll maximum (e.g., MacIntyre et al. 1999). In fact, this two-dimensional process likely occurred in Toolik Lake in 1999. Internal waves were generated by diurnal winds as L_N dropped below 10 and sometimes as low as 2 for periods of half a day. Internal wave displacements were larger at the Central Station, a site where the thermocline intersected the sloping bottom boundary of the lake, than at Toolik Main and were sufficient to bridge the distance between the nutricline and the chlorophyll maximum (Fig. 12). For the 21 microstructure profiles taken during the warming period at TM, 740 turbulent patches ($\varepsilon > 10^{-10}$ m^2 s^{-3}) were found within the metalimnion. Turbulence is an intermittent process (Thorpe 1977), so not all of the metalimnion was turbulent. In addition, due to the damping effects of viscosity and stratification, not all turbulent events induce transport (Itsweire et al. 1993; Saggio and Imberger 2001; Shih et al. 2005). Consequently, even when ε can be measured, K_z may be at molecular rates. For the turbulent patches identified at TM, 5% had K_z greater than molecular dissipation, and only 2% had values exceeding 10^{-5} m^2 s^{-1}. In contrast, the six microstructure profiles taken during the same period at the Central Station had 163 turbulent patches. In 21% of the patches, K_z exceeded molecular dissipation, and in 15% $K_z > 10^{-5}$ m^2 s^{-1}. The percentages were similar during the cooling period. These results indicate that mixing within the metalimnion was greater near the sloping boundaries of Toolik Lake and implies that near-boundary mixing is important for vertical transport in small lakes as has been observed in moderate-size to large lakes (Goudsmit et al. 1997; Saggio and Imberger 1998, 2001; MacIntyre et al. 1999).

We estimated the vertical flux of nutrients into the chlorophyll maximum as $F = K_z\ \partial C/\partial z$, and change in concentration (C) as $\partial C/\partial t = K_z\ \partial^2 C/\partial z^2$. Using our time series of lake-wide average K_z and measured gradients in mid-July in NH_4^+ of 0.04 mmol m^{-4} (μmol L^{-1} m^{-1}) and 0.07 mmol m^{-4} at 8 and 9 m, respectively, and a gradient in NO_3^- of 0.05 mmol m^{-4} at 9 m, the average daily flux of inorganic N was 0.006 mmol m^{-2} d^{-1} upward at 8 m and 0.012 mmol m^{-2} d^{-1} at 9 m in the heating period before the storm (days 180–198). Assuming that the nitrogen was mixed upward only 1 m, that typical primary production was 5 mg C m^{-3} d^{-1}, and that uptake of N and C followed Redfield ratios, these fluxes would have supported 10% and 22% of the required N per day between 7 and 8 m and between 8 and 9 m, respectively. During the heating periods, internal wave motions coupled with mixing at sloping boundaries is the primary pathway for vertical transport and supply of nutrients to the chlorophyll maximum. Because fluxes are low and nutrient regeneration rates apparently cannot meet demand, nutrient deficiency develops.

Pathways for nutrient flux during cooling and transition periods—As a result of sustained $L_N < 3$ on days 198–199, 201–202, and 210–212, internal waves increased in frequency and sometimes in amplitude, and during the latter two periods the metalimnion abruptly deepened (Figs. 5B and 12). Unfortunately the thermistor chain at the Central Station was pulled for downloading during the high winds on day 198 so that the full response at that site cannot be seen. The enhanced turbulence ($\varepsilon > 10^{-7}$ m^2 s^{-3}) between 6 m and the bottom at Central on day 199 (Fig. 10B), compared with very low values of $\sim 10^{-9}$ in the metalimnion away from the boundary, is an example of mixing near the benthic boundary due to the enhanced internal wave activity.

Several lines of evidence indicate that turbulence was induced not only in the metalimnion but also in the hypolimnion when $L_N \leq 3$. For example, ε was $>10^{-8}$ m^2 s^{-3} and sometimes exceeded 10^{-7} m^2 s^{-3} within the hypolimnion at

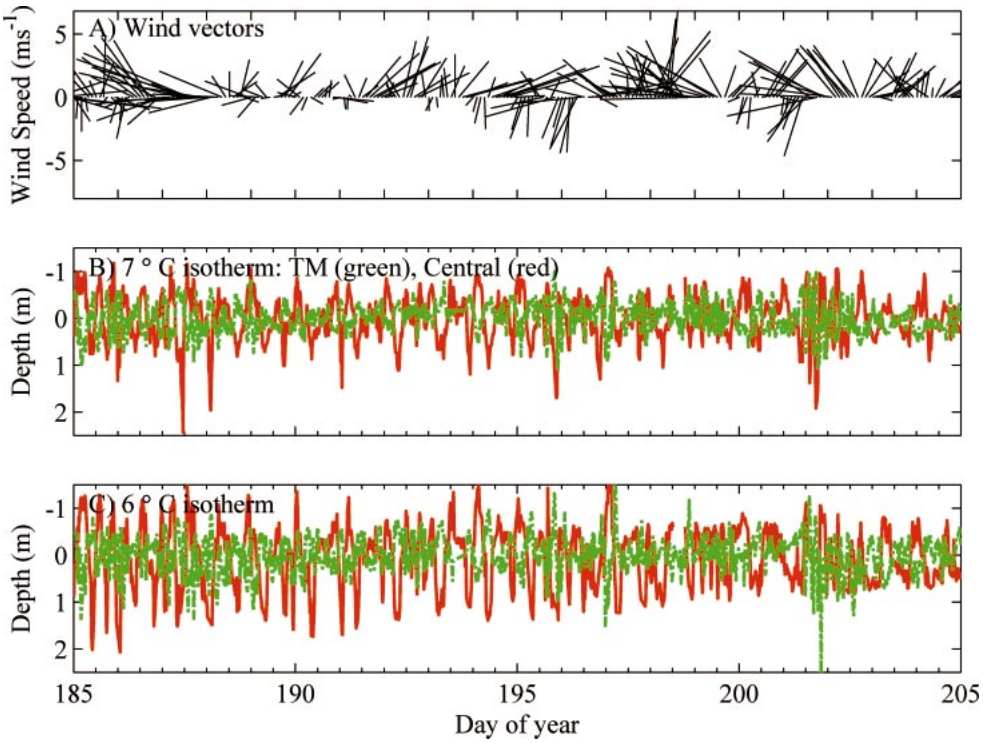

Fig. 12. (A) Time series of wind vectors with north vertical up, (B) detrended 7°C, and (C) detrended 6°C isotherms at TM (green) and Central Station (red) from day of year 185 to 205 showing larger amplitudes at Central Station, increasing frequency of isotherm displacements when $L_N < 3$ on days 199 and 201–202. From day 185 to day 205, 7°C isotherm descended from 6 m to 8 m and 6°C isotherm descended from 8 to 10 m. Isotherms were subsampled at 2-min intervals for ease of plotting.

TM on day 199 (Fig. 9B), and metalimnetic K_z was $>10^{-6}$ m^2 s^{-1} (Fig. 5C). The rate of heating increased in the hypolimnion at that time (Fig. 5B). Increased SC below 18 m on days 199–201, the movement of the 64 μS cm $^{-1}$ isocline from 20 m on day 196 to 11 m on day 199 (Fig. 6A), and increases in PC : PN (not shown) in bottom waters also provide evidence that near bottom mixing occurred when L_N dropped below 3. Additionally, NH_4^+ concentrations had increased by day 206 in the metalimnion and hypolimnion at depths below the intrusion (Fig. 11). Hence, mixing induced when $L_N \leq 3$ has the potential to entrain nutrients from the hypolimnion into the metalimnion.

Low L_N events also caused abrupt deepening of the mixed layer (Fig. 5B, day 212). Solutes or phytoplankton in the upper metalimnion would be mixed into the upper euphotic zone leading to the potential for increased primary productivity. For example, using $K_z = 9 \times 10^{-5}$ m^2 s^{-1} in the upper metalimnion (days 210–212, K_z calculated with a high-frequency cutoff of 3 d), a gradient of 0.05 mmoles m^{-4} in NH_4^+ (Fig. 11A), and assuming C uptake follows the Redfield ratio, the vertical flux of NH_4^+ would have been sufficient to support 31 mg C m^{-2} d^{-1}, 50% of the measured areal primary productivity on day 217. Cooling events themselves can lead to entrainment with important consequences. The cool air mass that arrived on day 208 was not accompanied by enhanced winds, yet it led to final entrainment of the plume waters into the epilimnion (Fig. 5B).

Stream inflows and fluxes—Loading of inorganic N from the stream during the storm for the 5 d beginning on day 197.5 was 2.4 mmol m^{-2} of lake surface. This quantity is equivalent to 40% of the loading that occurred in a low flow season (i.e., mid-May to the end of August; Whalen and Cornwell 1985). Due to temporal variation of insertion depths of the inflow (Figs. 5, 8–10, 11) and its nonuniform spatial distribution (Fig. 1), nutrient loading was variable over space and time. We quantified the loading into discrete layers using an import-dilution-advection approach with constraints provided by our observations from microstructure profiling and lake-wide sampling for SC and rhodamine. We first used the model for periods of falling discharge, as the rhodamine tracer could be used for validation. We then used it for the period of full discharge to calculate nutrient loading in various layers.

The approach for calculating loading and concentration in TIB is as follows. For time intervals of 2.7 and 6.7 h, which represent the transit time between TIB and TM during peak and falling discharge, we (1) computed the moles of solutes entering TIB from our loading measurements (Fig. 4), (2) added the number of moles already in the basin and subtracted the moles exiting from TIB assuming the solutes were well mixed and the discharge into the main basin equaled that flowing into TIB with a time lag based on flow speed into the main basin, and (3) calculated concentrations in TIB by dividing the remaining moles by the volume of TIB. We similarly calculated concentrations in layers in the main basin assuming a time lag of ~5.4 h for water to flow out of the main basin. The loading into discrete layers was calculated by dividing the moles entering TIB and TM each day by the volume of the layer into which the water flowed.

Table 1. Calculated nutrient loading into Toolik Inlet Bay and layers within the main basin of Toolik, daily carbon uptake due to combined increases in NO_3^- and NH_4^+ (C-uptake DIN) assuming uptake follows the Redfield ratio, and increase in primary productivity possible from DIN assuming a typical uptake rate is 20 mg C m^{-3} d^{-1} (Increase C uptake) for the large storm event (days 198.5–200.5). Stream water mixed with TIB water is assumed to be an overflow into the upper 6 m until day 195.5, then a metalimnetic intrusion between 2 and 8 m resulting in layers from 0 to 2 m (upper), 2 to 6 m (middle), and 6 to 8 m (lower) with different concentrations.

Location	Day	Loading NO_3^- (mmol m^{-3} d^{-1})	Loading NH_4^+ (mmol m^{-3} d^{-1})	C uptake DIN (C m^{-3} d^{-1})	Increase C uptake
TIB					
	198.5–199.9	0.87	4.17	423.4	21.2
	199.5–200.5	0.44	1.6	171.4	8.6
Main basin					
Overflow	198.5–199.5	0.28	1.43	144	7.2
Upper layer	199.5–200.5	0.44	2.18	220	11
Middle layer	199.5–200.5	0.69	3.17	324	16.2
Lower layer	199.5–200.5	0.25	0.99	103	5.2

During the period of falling discharge, we validated our model using the rhodamine tracer. Intrusive layering occurred between 3 and 6 m in the main basin. Calculated concentrations of rhodamine in TIB and between 3 and 6 m depth in the main basin were 0.05 and 0.01 μg L^{-1}, respectively. These calculated values are similar to the depth-integrated measured values at TIB and the measured values in the main basin, and thus validate our approach. When the period of full discharge is considered, overflow initially occurred in the upper 5–6 m followed by intrusive flow between 2 and 8 m, which extended north of the main northeast-southwest moraine. Modeled concentrations of NO_3^- in layers were between 0.05 and 0.08 μmol L^{-1}, and modeled concentrations of NH_4^+ were ~0.25 μmol L^{-1}. These values are in reasonable agreement with measured values (Fig. 11). Sensitivity analyses conducted by varying the overall area into which the discharge flowed, layer thickness, and the timing of water exiting the lake gave results within 20% of those computed here. The agreement between measured and calculated values at depths of the overflow and intrusion indicates that the model captured the essential features of the intrusion process and validates use of the import-dilution-export approach to calculate loading in discrete layers.

During the large storm event, the supply of DIN to TIB was ~20 times that required for growth in the upper water column on the first day of high discharge and ~10 times that required on the second day (Table 1). During the overflow into the upper 6 m on the first day at Toolik Main, supply was 7 times that required for growth; supply on the second day when an underflow developed exceeded requirements by ~10-fold in the upper layer, 16-fold in the middle layer, and fivefold in the lower layer. Because DIN supply greatly exceeded requirements of the phytoplankton, biological uptake is unimportant in the import-export-dilution model. The increased concentrations of SRP in the main basin (Fig. 11C) indicate loading of P also exceeded demand.

Discussion

During the ice-free season at Toolik Lake, high stream discharge and the passage of fronts with sustained high winds disrupted the strong thermal stratification setup by prior warming. Increased internal wave activity and mixing fragmented the chlorophyll maximum and ultimately mixed nutrients from hypolimnetic waters into the metalimnion. During the discharge event, the stream was initially an overflow and ultimately an underflow. The resulting intrusions created a layer of phytoplankton in the main basin originating from the inlet basin and from lakes upstream, a layer of organic matter likely of terrestrial origin, and a layer with elevated SRP. Introduced inorganic nitrogen was at least 10-fold in excess of phytoplankton requirements. High volumetric productivity occurred on the first day of the storm. The high loading from the stream and the increased nutrient gradient in the metalimnion due to the strong vertical mixing from low L_N events primed the upper water column for additional growth. The increase in primary productivity from 29 mg C m^{-2} d^{-1} when phytoplankton were nutrient-limited to 65 mg C m^{-2} d^{-1} 10 d after the storm likely reflects this priming.

Understanding the impact of storm events on lake dynamics requires consideration of the flowpath of the incoming stream waters and the percentage of a lake that is affected. Lakes are rarely well mixed, and the flowpaths of incoming waters are dependent on stream temperature, the initial extent of mixture of stream and lake waters, and the density stratification and hydrodynamics away from the inlet. Strong initial stratification, combined with time-dependent changes in depth of incoming solutes and particulates from streams (Fig. 11) and groundwater, set the stage for formation of layers with different chemical composition. Such layers may allow the development of communities with the potential for higher productivity or even different species assemblages, as recently observed in fjords and coastal waters (Alldredge et al. 2001; Lovejoy et al. 2002; McManus et al. 2003). Layers with different nutrient ratios may also restrict or enhance competitive interactions with respect to light and nutrients (Litchman 1998, 2000; Klausmeier and Litchman 2001) that could lead to dominance of different species at different depths. Such layers also serve as reservoirs of higher nutrient water that may support growth at a later time. Our results, as well as those from earlier tracer and acoustic studies (Fisher and Smith 1983; Imberger 1985) indicate that variations in inflow pathways and development of distinct water

layers, which in turn control chemical and biological heterogeneity, may be a common occurrence during summer stratification in lakes.

Whether layered structures with elevated biomass will develop depends on growth rates relative to the timescale for mixing (e.g., Knauer et al. 2000). In our study, layer formation was followed by a cool windy period that led to turbulence in the upper mixed layer and metalimnion, and the layering was muted within 5 d. However, if the high discharge period had been followed by a warm period with limited wind forcing, the layers would have persisted. Doubling time of phytoplankton in oligotrophic lakes is often on a timescale of 2 d (Kalff 2002; J.O. Sickman unpubl. data). Hence, the increased growth rates made possible by the increased nutrient loading can lead to increased biomass in layers and to greater spatial heterogeneity in primary production.

The effect of disturbances on primary production also depends on the degree of nutrient limitation of the phytoplankton. Levine and Whalen (2001) documented that most arctic lakes are limited by N alone or by both N and P. This study shows that P sufficiency persists longer than N sufficiency after ice-off, and N limitation develops more rapidly in the upper water column than in the chlorophyll maximum. Wind events and deep mixing can only supply nitrogen because of the low vertical gradient of phosphorus. Therefore, wind events occurring before cells are P-limited will help sustain productivity at moderate levels. Storm events with considerable rain will lead to both N and P loading and will likely have a greater impact than wind events alone.

Dimensionless indices developed to characterize the hydrodynamics of lakes (Imberger and Patterson 1990) provide a framework for assessing the interactions between physical forcing and chemical and biological impacts. Recent laboratory studies (Horn et al. 2001; Boegman et al. 2005) have shown increasing nonlinearity in the internal wave field with implications for turbulence production as the Wedderburn number (similar to L_N) decreases below 3.3. In this study, when warm air masses were prevalent and diel winds were induced by local heating and cooling, L_N was higher and reductions in L_N persisted for shorter periods. Under these conditions, turbulence can supply nutrients to phytoplankton in the chlorophyll maximum but not in the upper mixed layer. In consequence, phytoplankton deeper in the water column may be less deficient in N than phytoplankton in the upper water column, and productivity may be higher than in the overlying water (e.g., day 190, 9 mg C m^{-3} d^{-1}). The persistent stratification associated with high L_N also allows for the persistence of metalimnetic intrusions if rains occur and lead to high discharge. When $L_N < 3$ for periods of 12 h or longer, as occurs during the transition between different air masses, the enhanced turbulence can fragment the chlorophyll maximum and entrain nutrients from deeper in the water column into the metalimnion. Introduction of nutrient-replete phytoplankton and nutrients into the upper water column with higher light leads to the possibility of increased growth. It is thus possible to relate aspects of lake function such as productivity to hydrodynamics, and to relate hydrodynamics to weather patterns.

Changes in processes that regulate weather patterns (e.g., the dominant atmospheric wind patterns that determine frontal systems; Overland et al. 2002) co-occur in the Arctic with climate warming. Preponderantly warm years occur when pressure is anomalously low over the Arctic Ocean and high south of the Bering Strait. Cool years occur when anomalously high pressure occurs over the Arctic Ocean. As seen here, rapid transitions from cold to warm are nested within these annual regimes. The frequency of these transitions and associated physical forcing events will determine variations in nutrient loading and pathways of nutrient movement within a lake. Between-year differences in the frequency of these events may explain the high variance in previous measurements of primary productivity at Toolik Lake during the ice-free period (O'Brien et al. 1997) and the relative roles of internal and external loading (e.g., Shostell and Buckaveckas 2004). If the recent increased intensity of precipitation events associated with global change observed in some temperate regions (Kunkel et al. 1999) also occurs in the Arctic, then storm events and discharge into lakes may increase. Rainfall records (Arctic LTER data) show that summer rainfall at Toolik from 1988 through 1996 was significantly less ($p = 0.0029$) than from 1997 through 2004. Average cumulative rainfall for the 60-d period following ice-off was 110 ± 38 mm from 1988 through 1996 and 185.5 ± 46 mm from 1997 through 2004. The trend over time is significant (Kendall $\tau = 0.632$ with $p < 0.001$). Our study in 1999 was representative of the latter period with cumulative rainfall of 181 mm. Storms with discharge >15 m^3 s^{-1} and >8 m^3 s^{-1} occurred in 40% and 67%, respectively, of years from 1992 to 2004. Higher discharges associated with higher rainfall may lead to increased nutrient loading in metalimnetic intrusions and development of reservoirs of high nutrient water or nutrient replete phytoplankton that will help sustain productivity during the stratified period. High discharge events will also lead to increased loading of suspended solids and terrestrial organic matter, which would lead to increasingly light-limited conditions. The implications of climate change for productivity thus depend not only upon predicted warming and increased stratification that would reduce vertical mixing, but also upon the frequency of transitions between warm and cold air masses and the intensity of precipitation.

Overall, our results show that the frequency with which frontal systems move through a region, with the associated decreases in L_N and increases in stream discharge, determines the temporal variance in nutrient supply to a lake during open-water conditions. Spatial variability in nutrient pathways is induced by the degree of penetration of incoming streams and the vertical layering of intrusions. Persistence of these layers is made possible if warming occurs and L_N remains high. These temporal events, and the resulting layers and heterogeneous structure in the lake, can be loci of intense mixing or nutrient supply critically important for sustaining growth in oligotrophic lakes.

References

ALLDREDGE, A. L., AND OTHERS. 2002. Occurrence and mechanisms of formation of a dramatic thin layer of marine snow in a shallow Pacific fjord. Mar. Ecol. Prog. Ser. **233:** 1–12.

BOEGMAN, L., G. N. IVEY, AND J. IMBERGER. 2005. The energetics

of large-scale internal wave degeneration in lakes. J. Fluid Mech. **531:** 159–180.

BOLAND, K. T., AND D. J. GRIFFITHS. 1995. Water column stability as a major determinant of shifts in phytoplankton composition: Evidence from two tropical lakes in northern Australia, p. 89–99 *In* F. Schiemer and K. T. Boland [eds.], Perspectives in tropical limnology. SPB.

CHEN, C. T., AND E. J. MILLERO. 1977. The use and misuse of pure water PVT properties for lake waters. Nature **266:** 707–708.

COWLES, T. J., AND R. E. DESIDERIO. 1993. Resolution of biological microstructure through in situ fluorescence emission spectra. Oceanography **6:** 105–111.

CRUMP, B. C., G. W. KLING, M. BAHR, AND J. E. HOBBIE. 2003. Bacterioplankton community shifts in an Arctic lake correlate with seasonal changes in organic matter source. Appl. Environ. Microbiol. **69:** 2253–2268.

ENGLERT, J. P., AND K. M. STEWART. 1983. Natural short-circuiting of inflow to outflow through Silver Lake, New York. Water Resources Res. **19:** 529–537.

FEE, E. J. 1979. A relation between lake morphometry and primary production and its use in interpreting whole-lake eutrophication experiments. Limnol. Oceanogr. **24:** 401–416.

———, R. E. HECKY, G. W. REGEHR, L. L. HENDZEL, AND P. WILKINSON. 1994. Effects of lake size on nutrient availability in the mixed layer during summer stratification. Can. J. Fish. Aquat. Sci. **51:** 2756–2768.

———, J. A. SHEARER, E. R. DEBRUYN, AND E. U. SCHINDLER. 1992. Effects of lake size on phytoplankton photosynthesis. Can. J. Fish. Aquat. Sci. **49:** 2445–2459.

FISHER, H. B., E. J. LIST, R. C. Y. KOH, J. IMBERGER, AND N. H. BROOKS. 1979. Mixing in inland and coastal waters. Academic Press.

———, AND R. D. SMITH. 1983. Observations of transport to surface waters from a plunging inflow to Lake Mead. Limnol. Oceanogr. **28:** 258–272.

FOZDAR, F. M., G. J. PARKER, AND J. IMBERGER. 1985. Matching temperature and conductivity sensor response characteristics. J. Phys. Oceanogr. **15:** 1557–1569.

GOUDSMIT, G. H., F. PEETERS, M. GLOOR, AND A. WÜEST. 1997. Boundary versus internal mixing in stratified natural waters. J. Geophysical. Res. **102:** 27903–27914.

GUILDFORD, S. J., AND R. E. HECKY. 2000. Total nitrogen, total phosphorus, and nutrient limitation in lakes and oceans: Is there a common relationship? Limnol. Oceanogr. **45:** 1213–1223.

HOBBIE, J. E., M. BAHR, AND P. A. RUBLEE. 1999*a*. Controls on microbial food webs in oligotrophic arctic lakes. Arch. Hydrobiol. Spec. Issues Advanc. Limnol. **54:** 61–76.

———, AND OTHERS. 1999*b*. Impact of global change on the biogeochemistry and ecology of an Arctic freshwater system. Polar Research **18:** 207–214.

HOLMES, R. M., A. M. AMINOT, R. KÉROUEL, B. A. HOOKER, AND B. J. PETERSON. 1999. A simple and precise method for measuring ammonium in marine and fresh water ecosystems. Can. J. Fish. Aquat. Sci. **56:** 1801–1808.

HORN, D. A., J. IMBERGER, AND G. N. IVEY. 2001. The degeneration of large-scale interfacial gravity waves in lakes. J. Fluid Mech. **434:** 181–207.

IMBERGER, J. 1985. Thermal characteristics of standing waters: An illustration of dynamic processes, p. 7–29. *In* B. R. Davies and R. D. Walmsley [eds.], Perspectives in southern hemisphere limnology. DR. W. Junk.

———. 1998. Flux paths in a stratified lake: A review, p. 1–17. *In* J. Imberger [ed.], Physical processes in lakes and oceans. Coastal and estuarine studies, V. 54. American Geophysical Union.

———, AND J. C. PATTERSON. 1990. Physical limnology. Advances in Applied Mechanics **27:** 303–475.

ITSWEIRE, E. C., J. R. KOSEFF, D. A. BRIGGS, AND J. H. FERZIGER. 1993. Turbulence in stratified shear flows: Implications for interpreting shear-induced mixing in the ocean. J. Phys. Oceanogr. **23:** 1508–1522.

IVEY, G. N., J. IMBERGER, AND J. R. KOSEFF. 1998. Buoyancy fluxes in a stratified fluid. p. 377–388. *In* J. Imberger [ed.], Physical processes in lakes and oceans. Coastal and estuarine studies, V. 54. American Geophysical Union.

JAMES, W. F., AND J. W. BARKO. 1991. Littoral-pelagic phosphorus dynamics during nighttime convective circulation. Limnol. Oceanogr. **31:** 900–906.

JASSBY, A., AND T. M. POWELL. 1975. Vertical patterns of eddy diffusion during stratification in Castle Lake, California. Limnol. Oceanogr. **20:** 530–543.

JELLISON, R., AND J. M. MELACK. 2001. Nitrogen limitation and particulate elemental ratios of seston in hypersaline Mono Lake, California, USA. Hydrobiologia **466:** 1–12.

JOHNSON, K. S., R. L. PETTY, AND J. THOMSEN. 1985. Flow injection analysis for seawater micronutrients, p. 7–30. *In* A. Zirino [ed.], Mapping strategies in chemical oceanography. American Chemical Society, Advances in Chemistry Series No. 209.

KALFF, J. 2002. Limnology: Inland water ecosystems. Prentice Hall.

KILLWORTH, P. D., AND E. C. CARMACK. 1979. A filling-box model of river-dominated lakes. Limnol. Oceanogr. **24:** 201–217.

KLAUSMEIER, C. A., AND E. LITCHMAN. 2001. Algal games: The vertical distribution of phytoplankton in poorly mixed water columns. Limnol. Oceanogr. **46:** 1998–2007.

KLING, G. W., G. W. KIPPHUT, AND M. C. MILLER. 1992*b*. The flux of CO_2 and CH_4 from lakes and rivers in arctic Alaska. Hydrobiologia **240:** 23–36.

———, ———, M. M. MILLER, AND W. J. O'BRIEN. 2000. Integration of lakes and streams in a landscape perspective: The importance of material processing on spatial patterns and temporal coherence. Freshwater Biol. **43:** 477–497.

———, W. J. O'BRIEN, M. C. MILLER, AND A. E. HERSHEY. 1992*a*. The biogeochemistry and zoogeography of lakes and rivers in arctic Alaska. Hydrobiologia **240:** 23–36.

KNAUER, K., H. M. NEPF, AND H. F. HEMOND. 2000. The production of chemical heterogeneity in Upper Mystic Lake. Limnol. Oceanogr. **45:** 1647–1654.

KUNKEL, K. E., K. ANDSAGER, AND D. R. EASTERLING. 1999. Long-term trends in heavy precipitation events over North America. J. Climate **12:** 2513–2525.

LEVINE, M. A., AND S. C. WHALEN. 2001. Nutrient limitation of phytoplankton production in Alaskan arctic foothill lakes. Hydrobiologia **455:** 189–201.

LITCHMAN, E. 1998. Population and community responses of phytoplankton to fluctuating light. Oecologia **117:** 247–257.

———. 2000. Growth rates of phytoplankton under fluctuating light. Freshwater Biol. **44:** 223–235.

LOVEJOY, C., E. C. CARMACK, L. LEGENDRE, AND N. M. PRICE. 2002. Water column interleaving: A new physical mechanism determining protist communities and bacterial states. Limnol. Oceanogr. **47:** 1819–1831.

MACINTYRE, S. 1993. Vertical mixing in a shallow, eutrophic lake: Possible consequences for the light climate of phytoplankton. Limnol. Oceanogr. **38:** 798–817.

———, K. M. FLYNN, R. JELLISON, AND J. R. ROMERO. 1999. Boundary mixing and nutrient flux in Mono Lake, CA. Limnol. Oceanogr. **44:** 512–529.

———, AND R. JELLISON. 2001. Nutrient fluxes from upwelling and enhanced turbulence at the top of the pycnocline in Mono Lake, CA. Hydrobiologia **466:** 13–29.

———, AND J. R. ROMERO. 2000. Predicting upwelling, boundary

mixing, and nutrient fluxes in lakes. Verh. Internat. Verein. Limnol. **27:** 246–250.

———, ———, AND G. W. KLING. 2002. Spatial-temporal variability in mixed layer deepening and lateral advection in an embayment of Lake Victoria, East Africa. Limnol. Oceanogr. **47:** 656–671.

MCMANUS, M. A., AND OTHERS. 2003. Changes in characteristics, distribution and persistence of thin layers over a 48 hour period. Mar. Ecol. Prog. Ser. **261:** 1–19.

MILLER, M. C., P. SPATT, P. WESTLAKE, D. YEAKEL, AND G. R. HATER. 1986. Primary production and its control in Toolik Lake, Alaska. Arch. Hydrobiol. Suppl. **74:** 97–131.

MONISMITH, S. G. 1985. Wind-forced motions in stratified lakes and their effect on mixed-layer shear. Limnol. Oceanogr. **30:** 771–783.

———. 1986. An experimental study of the upwelling response of stratified reservoirs to surface shear stress. J. Fluid Mech. **171:** 407–439.

NEPF, H. M., AND C. E. OLDHAM. 1997. Exchange dynamics of a shallow contaminated wetland. Aquat. Sci. **59:** 193–213.

O'BRIEN, W. J., AND OTHERS. 1997. The limnology of Toolik Lake. *In* A. M. Milner and M. W. Oswood, [eds.], Freshwaters of Alaska. Ecological Studies, V. 119. Springer-Verlag.

OVERLAND, J. E., M. WANG, AND N. A. BOND. 2002. Recent temperature changes in the western Arctic during spring. J. Climate **15:** 1702–1716.

QUAY, P. D., W. S. BROECKER, R. H. HESSLEIN, AND D. W. SCHLINDLER. 1980. Vertical diffusion rates determined by tritium tracer experiments in the thermocline and hypolimnion of two lakes. Limnol. Oceanogr. **25:** 201–218.

ROBARTS, R. D., M. WAISER, O. HADAS, T. ZOHARY, AND S. MACINTYRE. 1998. Contrasting relaxation of phosphorus limitation due to typhoon-induced mixing in two morphologically distinct basins of Lake Biwa, Japan. Limnol. Oceanogr. **43:** 1023–1036.

ROUSE, W. R., AND OTHERS. 1997. Effects of climate change on the freshwaters of arctic and subarctic North America. Hydrol. Process. **11:** 873–902.

SAGGIO, A., AND J. IMBERGER. 1998. Internal wave weather in a stratified lake. Limnol. Oceanogr. **43:** 1780–1795.

———, AND ———. 2001. Mixing and turbulent fluxes in the metalimnion of a stratified lake. Limnol. Oceanogr. **46:** 392–409.

SCHINDLER, D. W., AND OTHERS. 1996. The effects of climate warming on the properties of boreal lakes and streams at the Experimental Lakes Area, northwestern Ontario. Limnol. Oceanogr. **41:** 1004–1017.

SENGERS, J. V., AND J. T. R. WATSON. 1986. Improved international formulations for the viscosity and thermal conductivity of water substance. Journal of Physical and Chemical Reference Data. **15:** 1291–1314.

SHIH, L. H., J. R. KOSEFF, G. N. IVEY, AND J. H. FERZIGER. 2005. Parameterization of turbulent fluxes and scales using homogeneous sheared stably stratified turbulence simulations. J. Fluid Mech. **525:** 193–214.

SHOSTELL, J., AND P. A. BUCKAVECKAS. 2004. Seasonal and interannual variation in nutrient fluxes from tributary inputs, consumer recycling and algal growth in a eutrophic river impoundment. Aquat. Ecol. **38:** 359–373.

SPIGEL, R. H., AND J. IMBERGER. 1980. The classification of mixed layer dynamics in lakes of small to medium size. J. Phys. Oceanogr. **10:** 1104–1121.

SQUIRES, M. M., AND L. F. W. LESACK. 2002. Water transparency and nutrients as controls of phytoplankton along a flood-frequency gradient among lakes of the MacKenzie Delta, western Canadian Arctic. Can. J. Fish. Aquat. Sci. **59:** 1339–1349.

STAINTON, M. P., AND M. J. CAPEL. 1974. Particulate phosphorus. p. 67–70. *In* M. P. Stainton and M. J. Capel [eds.], The chemical analysis of fresh water. Fisheries Research Board of Canada, Ottawa.

STEVENS, C. L., AND J. IMBERGER. 1996. The initial response of a stratified lake to a surface shear stress. J. Fluid Mech. **312:** 39–66.

STRICKLAND, J. D., AND T. R. PARSONS, [eds.]. 1972. A practical handbook of seawater analysis. 2nd ed. Fisheries Research Board of Canada, Ottawa.

STUMM, W., AND J. J. MORGAN. 1981. Aquatic chemistry, 2nd ed. Wiley.

THORPE, S. A. 1977. Turbulence and mixing in a Scottish loch. Phil. Trans. Roy. Soc. Lond. Ser. A **286:** 125–181.

VINCENT, W. F., M. M. GIBBS, AND R. H. SPIGEL. 1991. Eutrophication processes regulated by a plunging river inflow. Hydrobiologia **226:** 51–63.

———, AND J. E. HOBBIE. 2000. Ecology of arctic lakes and rivers, p. 197–232. *In* M. Nuthall and T. V. Callaghan [eds.], The Arctic: Environment, people, policy. Academic.

WETZEL, R. G., AND G. E. LIKENS. 2000. Limnological analyses, 3rd ed. Springer.

WHALEN, S. C., AND V. ALEXANDER. 1984. Influence of temperature and light on rates of inorganic nitrogen transport by algae in an arctic lake. Can. J. Fish. Aquat. Sci. **41:** 1310–1318.

———, AND ———. 1986. Seasonal inorganic carbon and nitrogen transport by phytoplankton in an arctic lake. Can. J. Fish. Aquat. Sci. **43:** 1177–1186.

———, AND J. C. CORNWELL. 1985. Nitrogen, phosphorus, and organic carbon cycling in an arctic lake. Can. J. Fish. Aquat. Sci. **42:** 797–808.

WÜEST, A., G. PIEPKE, AND J. D. HALFMANN. 1996. *In* T. C. Johnson and E. O. Odada [eds.]. The limnology, climatology and paleoclimatology of the East African Lakes. Gordon and Breach Scientific.

YEATES, P. S., AND J. IMBERGER. 2004. Pseudo two-dimensional simulations of internal and boundary fluxes in stratified lakes and reservoirs. Intl. J. River Basin Management **1:** 1–23.

Received: 18 January 2005
Accepted: 9 September 2005
Amended: 12 October 2005